



universität  
wien

# DIPLOMARBEIT

Titel der Diplomarbeit

Preparation and optimization of PLGA Nanoparticles loaded with Cholesterol:  
formulative and technological parameters

Verfasserin

Birgit Gstötenbauer

angestrebter akademischer Grad

Magistra der Pharmazie (Mag.pharm.)

Wien, 2013

Studienkennzahl lt.  
Studienblatt:

A 449

Studienrichtung lt.  
Studienblatt:

Pharmazie

Betreuer:

a.o. Univ. Prof. Mag. Dr.Franz Gabor



## **Vorwort**

Die experimentellen Untersuchungen zur vorliegenden Arbeit wurden am Department für pharmazeutische Technologie und Nanomedizin der Universität Modena im Zeitraum von März 2012 bis Juni 2012 unter der Anleitung von Dr. Giovanni Tosi im TeFarTI Research Center durchgeführt.

An dieser Stelle möchte ich mich bei ihm und Dr. Daniela Belletti, die mich während der gesamten Zeit betreut hat, für die Aufnahme in ihre Arbeitsgruppe und die interessante Themenstellung bedanken.

Weiters danke ich a.o. Univ. Prof. Mag. Dr. Franz Gabo r für die Möglichkeit, meine Diplomarbeit im Ausland zu absolvieren und für die Unterstützung und Betreuung nach meiner Rückkehr.

Ein besonderer Dank gilt Mag. Eva Maria Wirth, die mir vom ersten bis zum letzten Tag meines Studiums immer zur Seite stand.

Zu guter Letzt möchte ich mich bei meiner Familie bedanken, die mir nicht nur dieses Studium ermöglicht hat, sondern mich auch während der gesamten Zeit großartig unterstützt hat.



# TABLE OF CONTENTS

<b>1. INTRODUCTION</b>	<b>7</b>
<b>1.1. CENTRAL NERVOUS SYSTEM (CNS)</b>	<b>7</b>
1.1.1 BBB STRUCTURE AND FUNCTION	8
1.1.2. STRUCTURE AND CELL TYPES OF THE BLOOD-BRAIN BARRIER	8
1.1.3 TIGHT JUNCTIONS	9
1.1.4 TRANSPORT ACROSS THE BBB	10
1.1.5 PROBLEMS AND THEORIES OF ADMINISTRATION TO THE BRAIN	12
<b>1.2. NANOPARTICLES (NPs)</b>	<b>13</b>
1.2.1. FUNCTIONALIZED NPS	15
<b>1.3. CHOREA HUNTINGTON</b>	<b>15</b>
1.3.1 SYMPTOMS	16
1.3.2 GENETICS	17
1.3.3 THERAPIES FOR HD	18
<b>1.4. CHOLESTEROL IN THE BRAIN</b>	<b>19</b>
1.4.1 BRAIN CHOLESTEROL IN HUNTINGTON'S DISEASE	21
1.4.2. IIN VITRO OR IN VIVO ATTEMPTS FOR CHOLESTEROL RESCUE	23
<b>2. AIM OF THE WORK</b>	<b>24</b>
<b>3. MATERIALS</b>	<b>25</b>
1. POLY(LACTIC-CO-GLYCOLIC ACID)	25
2. CHOLESTEROL	27
3. POLYVINYL ALCOHOL	28
4. ACETONE	29
5. D-(+)-TREHALOSE DIHYDRATE	30
6. GLUCOSE	31
7. D-SORBITOL	32
8. D-MANNITOL	33
9. ETHANOL, ABSOLUTE	34
10. CHLOROFORM	35
11. ISOPROPYL ALCOHOL	36
12. ACETONITRILE	37
<b>4. METHODS</b>	<b>38</b>
<b>4.1. PREPARATION OF NP</b>	<b>38</b>
4.1.1 NANOPRECIPITATION	38
4.1.2. PURIFICATION AND COLLECTION OF THE NANOPARTICLES	39
<b>4.2. CHARACTERIZATION OF NANOPARTICLES</b>	<b>39</b>
4.2.1. MORPHOLGY OF NANOPARTICLES	39
4.2.2 SIZE AND ZETA POTENTIAL OF NANOPARTICLES	40
4.2.3. ZETA-POTENTIAL MEASUREMENT	41
4.2.4. RECONSTITUTION OF LYOPHILIZED NANOPARTICLES	43
4.2.5. DETERMINATION OF ENTRAPMENT EFFICIENCY	43
<b>5. RESULTS</b>	<b>47</b>
<b>5.1. CHARACTERIZATION OF CHOLESTEROL-LOADED RESOMER®503- Nps</b>	<b>47</b>
5.1.1 PHYSICO-CHEMICAL CHARACTERIZATION OF CHOLESTEROL-LOADED RESOMER®503- Nps	48
5.1.2 MORPHOLOGICAL CHARACTERIZATION OF 5 CHOLESTEROL-LOADED RESOMER®503- Nps	50
5.1.3 ENCAPSULATION EFFICIENCY OF CHOLESTEROL-LOADED RESOMER®503- Nps	53

5.1.4 INFLUENCE OF TYPE AND AMOUNT OF CRYOPROTECTANT ON CHOLESTEROL-LOADED RESOMER®503- NPs	55
<b>5.2. STRATEGIES TO IMPROVE THE CHOLESTEROL RELEASE FROM CHOLESTEROL-LOADED RESOMER®503- NPs</b>	<b>57</b>
5.2.1. ADDITION OF SUCROSE DURING MATRIX FORMATION	57
5.2.2. FORMULATION AND PHYSICO-CHEMICAL CHARACTERIZATION OF SUGAR-MODIFIED CHOLESTEROL-LOADED RESOMER® 503 NPs	58
5.2.3 CHOLESTEROL-CONTENT OF SUGAR-MODIFIED CHOLESTEROL-LOADED RESOMER® 503 NPs	61
5.2.4. USE OF LOW MOLECULAR WEIGHT PLGA	61
<b>6. DISCUSSION</b>	<b>64</b>
<b>7. REFERENCES</b>	<b>69</b>
<b>8. DEUTSCHE ZUSAMMENFASSUNG</b>	<b>72</b>
<b>9. CURRICULUM VITAE</b>	<b>74</b>

# 1. Introduction

## 1.1. Central Nervous System (CNS)

35% of human diseases with high impact on health affect the brain and are generally characterized by a rapid and lethal progress (Chen et al., 2012).

The disorders, which mostly affect the brain, are tumors, ischemia and neurodegenerative diseases such as Alzheimer, Parkinson and M. Huntington (Wohlfart et al., 2012). All these pathologies are characterized by a loss of one or more functions of the CNS.

Many of the above mentioned diseases are not yet fully understood because different triggers like genetic factors, oxidative stress, inflammations, protein aggregations and others may be involved in neurodegenerative damage and their development.

The number of people suffering from any kind of neurodegenerative disease is increasing constantly leading to an increased need for a treatment, which is not only improving the symptoms but also aiming to treat the cause. Many therapies used recently do not display the best pharmacokinetic, biopharmaceutical and toxicological profile leading to a non-efficient therapy. This is not because of the lack of possible drugs but due to the inability of many therapeutic molecules to cross the blood brain barrier (BBB) (Chen et al., 2012).

Many drugs, even if they are more active, potent or useful in treating brain cancers, HIV-dementia, strokes, ischemia, Alzheimer and Parkinson's diseases if compared to those which are actually applied in clinical treatments, are not able to cross the blood brain barrier (BBB) in therapeutic doses. (Chen et al., 2012)

This shows one of the biggest limitations of existing therapies and the reason for the failure of many pre-clinical and clinical studies (Tosi, Costantino, 2007). The non achieved therapeutic dosage of applied agents in the central nervous system (CNS) limits the non-invasive therapies (Wong et al., 2012). Therefore, one of the most significant challenges facing CNS drug development is the availability of an effective brain targeting technology (Wong et al., 2012). The carriers must be designed that way that the drugs can be delivered to the target sites at the right time at an optimal level and with appropriate release kinetics (Wong et al., 2012). Nanotechnology is among the most frequent used approaches for approaching this problem. Nanoparticles, polymeric nanoparticles,

liposomes, nanoemulsions, nanogels or nanosuspensions and many more are just some of the nanotechnologies used for delivering drugs to the CNS. (Vinogradov et al., 1999; Shubar et al., 2009)

Till today there is still no „perfect“ nanocarrier found yet. (Wong et al., 2012)

### **1.1.1 BBB structure and Function**

The BBB represents the border between circulating blood from the brain and extracellular fluid (BECF) in the central nervous system (CNS). It exists along all capillaries and consists of endothelial cells and tight junctions around the capillaries that are not present in normal circulation. The cells of the BBB actively transport metabolic products (e.g. glucose) across the barrier with specific proteins. This barrier also includes a thick basement membrane and astrocytic endfeet.

The functions of the blood brain barrier (BBB) are to protect the brain against toxic compounds, to control the brain homeostasis by controlling the ions concentration and to regulate the transport between blood and brain compartments.

The BBB is a selective barrier, which can differentiate between needed substances, like nutrients, or toxic substances. The BBB is present in all brain regions, except those, which regulate the autonomic nervous system and endocrine glands of the body. In these areas, blood borne molecules can diffuse through fenestrations in blood vessels (Allah, Braun et al. 2004).

### **1.1.2. Structure and cell types of the blood-brain barrier**

The BBB is necessary to provide an optimal chemical environment for cerebral function. Several layers exist between blood and brain consisting mainly of three different cell types: capillary endothelial cells (ECs), a basement membrane consisting of type IV collagen, pericytes embedded in the basement membrane and astrocyte processes that surround the basement membrane.

For the neuronal function astrocytes are very important. They are able to enhance the charge selectivity of ECs by increasing the production of proteoglycan, which forms the



negatively charged glycocalyx (Abbott, Patabendige et al. 2010; Cardoso, Brites et al. 2010). The close association between ECs and astrocytes is highly important for the function of the BBB (Abbott, Patabendige et al. 2010).

Pericytes are mainly needed for the proliferation and also differentiation of endothelial cells and they can also change the permeability of the BBB.

In critical situations, such as hypoxia, pericytes are able to dissociate from the micro vessels and so the transport across the BBB increases (Hawkins & Davis 2005).

### **1.1.3 Tight Junctions**

Key features of the BBB are tight junctions (TJ), which keep macromolecules and polar solutes from entering the brain (Abbott, Patabendige et al.. 2010). TJ are located in the apical area of the ECs and they mainly influence the properties of the BBB (Cardoso, Brites et al. 2010); they build a strong barrier made of connected ECs without any gaps or spaces in between the cells. These structures make sure that only a limited number of molecules can pass the BBB, like O<sub>2</sub> and CO<sub>2</sub>.

The complex structure of TJ is formed by various proteins, such as transmembrane proteins like occludin and claudin (Abbott, Patabendige et al.. 2010).

Additionally there are adherent junctions, which are located below the TJ. They are of great importance for the formation of TJ by providing structural support and keeping cells together (Abbott, Patabendige et al. 2010; Cardoso, Brites et al., 2010). Adherent junctions are formed by Cadherin, a Ca<sup>2+</sup>-dependent transmembrane protein, which is linked to a protein of the catenin family (Cardoso, Brites et al., 2010) that is able to build a complex with the actin filaments on the surface of ECs, forming a bridge between two cells (Cardoso, Brites et al., 2010).

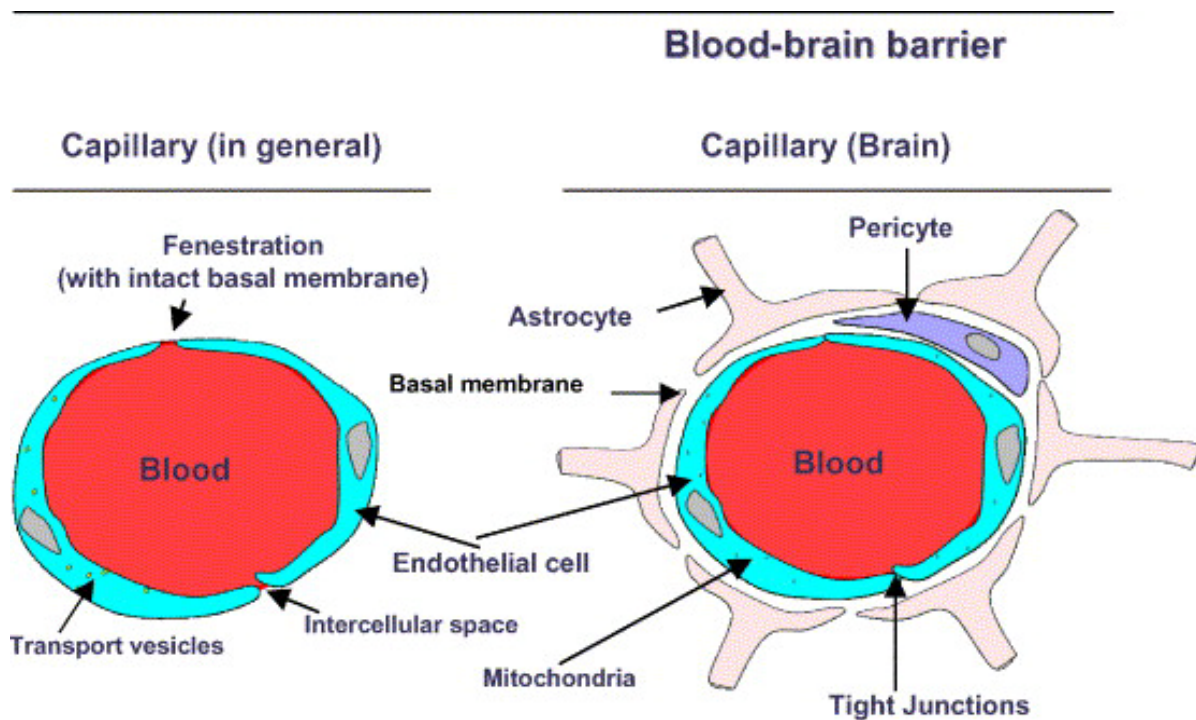


Fig.1.1.: Comparison of a „normal“ blood capillary to a brain capillary. Differences are seen in the presence of astrocytes, pericytes, tight junctions, mitochondria and the missing fenestrations in the brain capillary. (Figure from Löscher et al., 2005)

#### 1.1.4 Transport across the BBB

The function and structure of the BBB prevents a great number of compounds and nutrients from entering the CNS easily. Blood gases,  $O_2$  and  $CO_2$  benefit from their concentration gradients to enter the CNS. Passive diffusion is the uptake mechanism for small, unipolar and lipid soluble molecules and ethanol.

Small molecules can use the paracellular pathway to cross the BBB, charged and polar molecules have to be transported via the transcellular pathway (Petty & Lo, 2002).

Solute carriers, present in ECs of the BBB, facilitate the transport of polar compounds, such as glucose or amino acids to the CNS. Furthermore, small peptides, free fatty acids, organic anions and cations are also transported by solute carriers (Abbott, Patabendige et al., 2010).

Depending on the direction of the transportation – from blood to brain or vice versa – solute carriers are either on one side only or on both sides, which means either luminal, abluminal or at both membranes of ECs (Abbott 2002; Bernacki, Dobrowolska et al., 2008).

Glucose transporter-1, called GLUT-1, ensures sufficient supply of glucose, the main energy source of the CNS. (Persidsky, Ramirez et al., 2006).

Besides supporting the CNS with essential nutrients, specific transporters in the BBB protect the brain from toxic and noxious substances by actively pumping them out of the brain compartment (Abbott, Patabendige et al., 2010).

In order to transport compounds actively out of the CNS, ATP-dependent ABC-transporters are used (Abbott, Patabendige et al. 2010). The substrates for ABC-transporters are lipid-soluble compounds, such as neurotoxic molecules, whose removal protects the functions of the brain. Moreover, many drugs can be actively effluxed out of the brain. So simply increasing the lipid solubility of a drug does not guarantee penetration into the brain (Dauchy, Dutheil et al. 2008; Abbott, Patabendige et al. 2010).

Macromolecules, such as proteins or peptides (albumin, insulin, low density lipoproteins) cross the BBB via endocytotic mechanisms. There are two types of transcytosis: receptor-mediated (RMT) or absorptive mediated transcytosis (AMT). Both mechanisms make sure that macromolecules can cross the BBB (Abbott, Patabendige et al. 2010).

Endocytosis or transcytosis allow the internalization, sorting and trafficking of many plasma macromolecules. (Wong et al., 2012)

The process, which internalizes molecules from the circulation into vesicles and delivers them to endosomes or lysosomes within the cell, is called endocytosis; Transcytosis refers to the transcellular movement of molecules (Wong et al. 2012).

Adsorptive endocytosis or transcytosis is used by high molecular weight substances proteins (IgG, histone, albumin, native ferritin, dextran). Adsorptive processes depend on electrostatic interactions that allow the normally positively charged substrate to bind to the negatively charged cell membrane (H.L. Wong et al. 2012),

Receptor-mediated processes are activated by ligand-binding to luminal cell-surface receptors which lead to internalization of the receptors at the luminal side followed by either endocytosis into endosomes or lysosomes or transcytosis across the membrane to

be externalized at the abluminal surface (M. Simionescu et al, 2002).

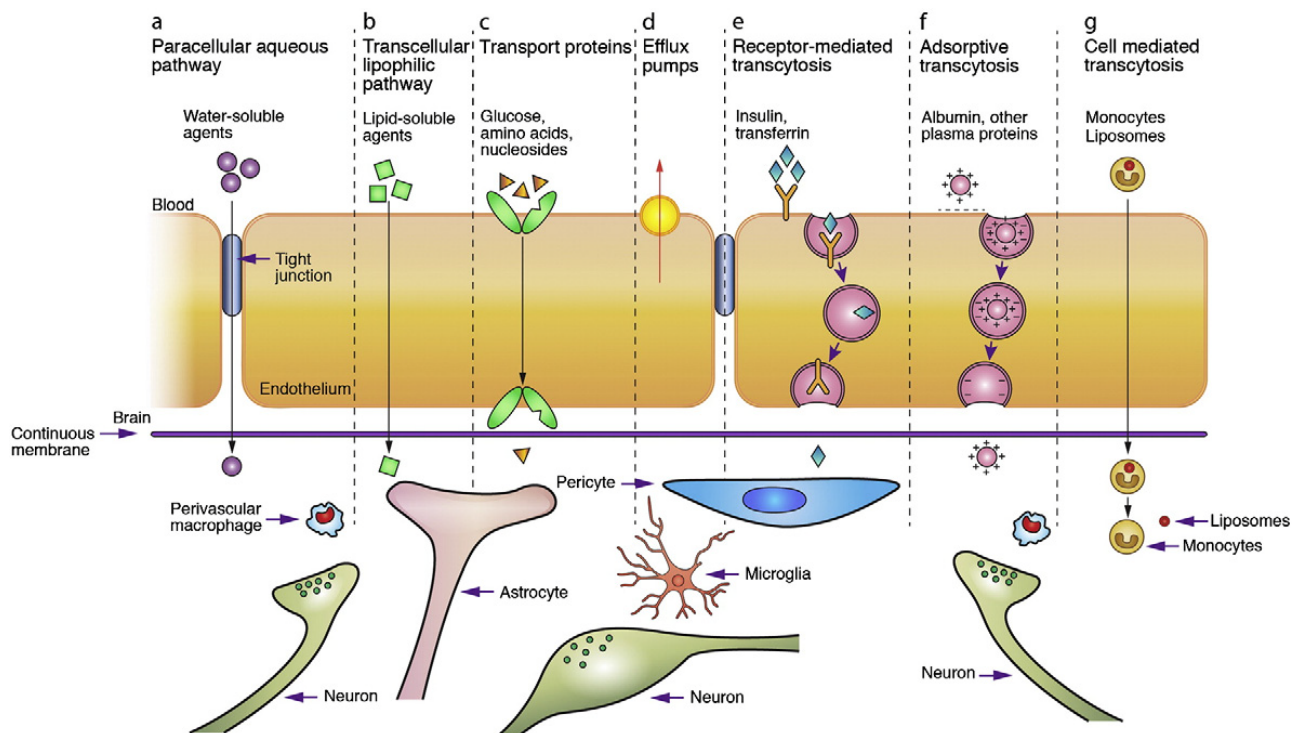


Fig.1.2 Transport routes across the blood–brain barrier. Pathways “a” to “f” are common for solute molecules; and the route “g” involves monocytes, macrophages and other immune cells and can be used for any drugs, drug-incorporated liposomes or nanoparticles. (Chen, et al, 2012; Abbott, et al, 2006)

### 1.1.5 Problems and theories of administration to the brain

Besides the above-mentioned difficulties related to BBB pathophysiological features, the main problems concerning the treatment of CNS diseases are connected to several drawbacks of the drugs themselves:

- the distribution of the active substances over the whole body
- the need to administer high dosages to reach a sufficient concentration in the brain
- the adverse effects due to the high dosage
- the lack of specific transport systems across the BBB
- the presence of efflux systems (i.e. P-glycoprotein)

Therefore, many studies were dealing with the problem of specific drug delivery to the brain. Some approaches that are used are:

**a) invasive techniques** used in neurosurgery: the active substance is directly injected into the brain. This technique is efficacious but often decreases the patient's compliance, also considering the risk of infections due to the surgical intervention.

- Infusions, catheters, microchips, polymeric systems
- temporary „breaking“ of the tight junctions and use of hyperosmotic solutions.

**b) Non-invasive techniques** with probable higher compliance for patients and especially useful in chronic illness.

- Biological approach: conjugation with antibodies
- Chemical approach: prodrugs, inclusion bodies
- Technological approach: nanoparticles, liposomes, solid lipid nanoparticels.

## 1.2. Nanoparticles (NPs)

Nanoparticles are among the most studied drug delivery systems due to their ability to entrap, stabilize, and deliver different types of active substances. They are defined as particles with a diameter ranging from a few to 500 nanometers (Sung-Wook et al., 2003). They can encapsulate both hydrophilic and lipophilic drugs and protect them from enzymatic degradation after administration. (Sung-Wook et al., 2003). For the preparation of micro- and nanoparticles, synthetic polymers such as polyesters (poly-(D, L)) glycolic acid, poly- (D, L) lactic acid poly  $\beta$ -hydroxybutyric acid, poly (lactic-co-glycolic acid) and the poly  $\epsilon$ -caprolactone), polyanhydrides, and polycyanoacrylates are mostly used. There is also the possibility of using natural polymers such as proteins (albumin and gelatin) and polysaccharides (chitosan and alginates), which, although often less toxic, suffer from the disadvantage of low stability due to more easily degradation by plasma enzymes such as hydrolases.

Among the most widely used synthetic polymers is the PLGA (polylactic-co glycolic acid), which is approved from both the Food and Drug Administration (FDA) and the European Medicine Agency (EMA) for parenteral administration (Danhier et al., 2012). This polymer, compared to natural polymers, is less degradable by enzymes that are present in the

blood circulation (like hydrolases) and is, therefore, more stable.

Surface charges of nanoparticles also exert important influence on their interaction with cells and on their uptake (Danhier et al., 2012). Positively charged nanoparticles seem to promote a higher level of internalization, apparently as a result of the ionic interactions between positively charged particles and negatively charged cell membranes (C. Foged et al, 2005; J.K. Vasir et al, 2008),

In order to develop long-term active formulations, in which sensitive drugs could be delivered to their target without degradation, a variety of active compounds has been encapsulated into PLGA micro- and nanoparticles (Mundargi et al., 2008), e.g. recombinant human growth factor (Rafi et al., 2010), porcine insulin (Bao et al., 2006), recombinant glycosylated glial cell-line derived neurotrophic factor (Garbayo et al., 2008), and HIV peptides (Manocha et al., 2005).

Nanometric systems can be divided into nanocapsules and nanospheres according to the technique of preparation used. In nanocapsules the active substance is largely encapsulated in the internal cavity of the particles (aqueous core), while in nanospheres it is finely dispersed in the polymer matrix.

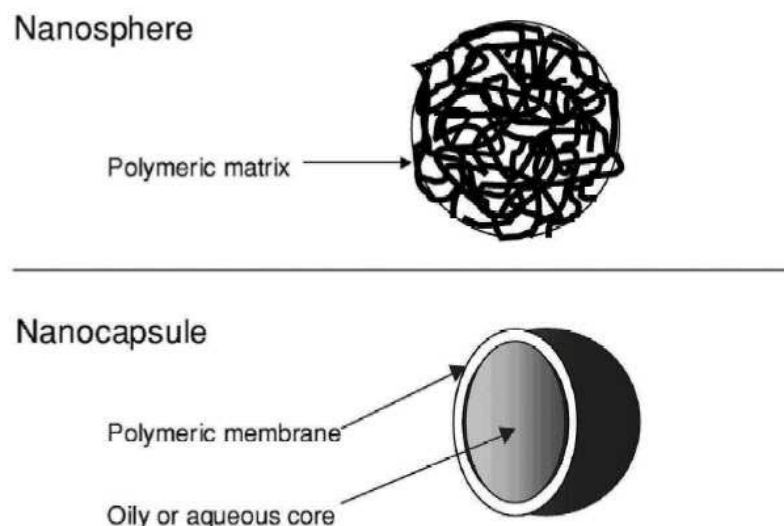


Fig. 1.3.: Schematic image of nanosphere compared to nanocapsule

NPs used in nanomedicine must be biocompatible, non-toxic, and biodegradable and they should not cause side effects. To fulfill these requirements the NPs should have a diameter close to 100nm. Moreover, a hydrophilic surface (typically a PEG coverage)

could preserve NPs from the opsonisation and an uptake by the reticuloendothelial system (RES).

NPs are also used for drug targeting, meaning the possibility of specifically directing the NPs to a specific cell population. This strategy comprises surface engineering of the NPs, typically by the conjugation with cell-specific ligands (peptides, antibodies). Thus, increasing the accumulation of the drug at the site of action, it might be possible to reduce the amount of active substances required for the therapeutic effect.

Besides the aim of targeting specific pathological sites (cells or organs), this strategy of NPs surface engineering could be also applied to cross virtually non-penetrable barriers, such as the BBB.

This could be obtained by using specific ligands (antibody/proteins), which support BBB crossing by taking advantage of BBB transport pathways such as receptor/non-receptor BBB endocytosis, or transcytosis.

### **1.2.1. Functionalized NPs**

Several in vivo studies demonstrated that modified polymeric nanoparticles prepared from a recently approved poly (D, L-lactide-co-glycolide) functionalized with glycopeptides (g7-NPs) cross the BBB and deliver drugs into the CNS (Tosi et al., 2007; Constantino et al., 2005; Tosi et al., 2011; Vergoni et al., 2009; Tosi et al., 2010). Starting from these findings, it was tried to optimize the technological parameters in order to prepare functionalized polymeric nanoparticles (Nps) with an efficient encapsulation of cholesterol and the ability to modulate the drug release, in vitro and in vivo.

### **1.3. Chorea Huntington**

Chorea Huntington (HD; Huntington's disease) is a neurodegenerative genetic disorder. The Huntington mutation leads to widespread brain neurodegeneration, with cell loss mainly in the striatum and cerebral cortex (Reiner et al., 1988), although neuronal abnormalities are also found in many other brain regions (Rosas et al., 2003).

The causes for HD are not fully understood but results from various studies suggest that

the brain-derived neurotrophic factor (BDNF) might contribute to the development of this disease. (Zuccato et al., 2007)

BDNF is a small dimeric protein that is widely expressed in the adult mammalian brain and has been shown to promote the survival of all major neuronal types affected in Alzheimer's disease and Parkinson's disease. (Zuccato et al., 2007)

Furthermore, cortical BDNF production is required for the correct activity of the corticostriatal synapse and the survival of the GABA-ergic medium-sized spiny striatal neurons that die in HD (Zuccato et al., 2007).

The disease is caused by an autosomal dominant mutation. This means that children of affected patients have a 50% chance of inheriting the disease.

The prevalence worldwide of HD is 1-2 cases per 20000 persons without significant differences between genders but among geographical locations.

The highest rate of HD is in Western Europe and, more precisely, there are some areas with a much higher prevalence, e.g. Lake Maracaibo in Venezuela, Tasmania, Scotland, Wales, and Sweden.

### **1.3.1 Symptoms**

The first symptoms usually start around the age of 40 years; changes in mood or cognition can be noticed at the beginning. These symptoms are later followed by coordination and psychiatric problems, which lead to a stage where coordinated movements become very difficult and mental problems can be diagnosed, such as dementia (Cattaneo, Zuccato et al., 2005).

The life expectancy after the onset of the first symptoms is around 15 years because of many complications such as pneumonia, heart disease and physical injury from falls coming along with the HD (Cattaneo, Zuccato et al., 2005).

Until today, there is no cure for HD, and full-time care is required in the later stages of the disease. However, there are therapies that can reduce the symptoms.



### 1.3.2 Genetics

The protein causing HD is called huntingtin. Huntingtin is essential for embryogenesis, and ubiquitously expressed at moderate amounts inside and outside the nervous system (Cattaneo, Zuccato et al., 2005)

The gene, which encodes this protein, is on the small arm of chromosome number 4. The gene mutation causes an expanded CAG tract mainly caused by „slippage“ (DNA polymerase slipped during replication) or by cross over. Healthy persons have 9 to 35 triplets of CAG, people with HD have 36 up to 250 CAG triplets. The more CAG triplets the sooner the disease will start. More than 60 repetitions lead to a start of the disease during childhood.

People with triplet repetitions from 36 up to 40 are an exception concerning the penetration, which means that not all of them will develop HD-symptoms. The normal penetration rate of HD is 100%.

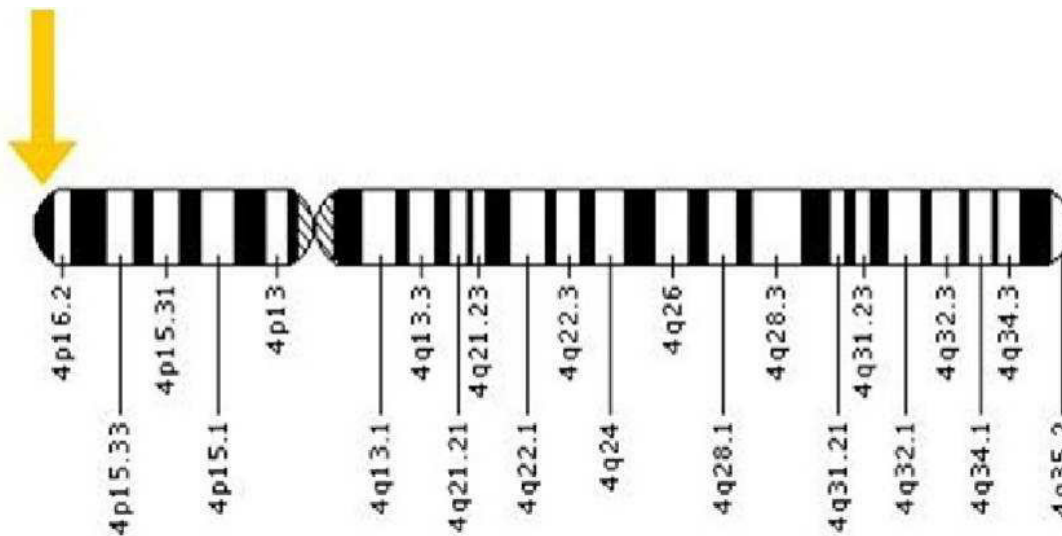


Fig. 1.4: Chromosome number 4 encodes a specific aminoacid: glutamine.

The expanded CAG tract (>35 repeats) at the 5' end is translated into a corresponding poly-glutamine stretch (polyQ) that makes medium spiny neurons in the striatum particularly vulnerable to cell death, and also leads to the dysfunction and death of neurons in other brain regions, including the cortex (Cattaneo, Zuccato et al., 2005).

The glutamines repeat extension of the huntingtin gene has been well documented in association with HD, but until now the huntingtin protein function remains unknown

(VanGilder et al., 2011). More recently, it has been suggested that the loss of normal huntingtin function might also contribute to the pathogenesis of HD (Cattaneo, Zuccato et al., 2005).

### **1.3.3 Therapies for HD**

The therapy of HD is difficult due to the lack of understanding of the disease and to the difficulty in delivering efficacious drugs to the site of action. The gap in knowledge limits current treatment options to focus on symptomatic relief of depression, psychosis, and chorea (involuntary writhing movement) (VanGilder et al., 2011). Chorea, one of the most difficult symptoms to treat, has recently been managed with tetra-benazine (TBZ), which is an antipsychotic medication (Fasano et al., 2008; Frank et al., 2008). TBZ promotes neurotransmitter degradation by preventing re-uptake of monoamine neurotransmitters (MAO) into presynaptic vesicles (Ondo et al., 1999). Even though TBZ is one of the few drugs available for treating chorea and has fewer side effects than the analogous drug reserpine (Kenney et al., 2007), neuron-focused medications do not halt disease progression.

Recent studies about the lack of BDNF has aroused interest in BDNF and/or BDNF mimetics as potential therapeutic agents, and this has been fostered by reports of reduced BDNF levels in the cerebral cortex and striatum of people with HD (Zuccato et al., 2001),

Psychiatric symptoms, like depression, are treated with selective serotonin re-uptake inhibitors. For psychosis and behavioral problems atypical antipsychotic drugs are mostly used.

Weight loss and eating difficulties have to be treated as well. High caloric food or adding thickening agents to liquids can alleviate the problems.

At a certain point nutrition management becomes an important issue due to dysphagia and other muscle disorders. If normal eating becomes uncomfortable or too dangerous because of aspirating food, percutaneous endoscopic gastrostomy is needed. This is done with a tube that leads directly to the stomach.

Breath exercises, walking aids and a psychotherapy can complete the symptomatic therapy.

#### 1.4. Cholesterol in the brain

Although it represents only 2% of the total body mass, the CNS is the most cholesterol-rich organ, containing 23% of the whole body cholesterol. (Wilson [et al.](#), 1968)

Brain cholesterol is an essential component of cell membranes, and is involved in a number of biological functions such as membrane trafficking, signal transduction, myelin formation and synaptogenesis (Valenza, Cattaneo [et al.](#), 2006). Given these widespread activities and the knowledge that all brain cholesterol derives from local synthesis, it is not surprising that dysfunctions in cholesterol synthesis, storage, transport and removal may lead to human brain diseases (Valenza, Cattaneo [et al.](#), 2006).

Consequently, high cholesterol levels are essential for myelin membrane growth *in vivo*. Therefore, it is not surprising, that mice that are unable to synthesize cholesterol properly develop ataxia and tremor (Saher [et al.](#), 2005).

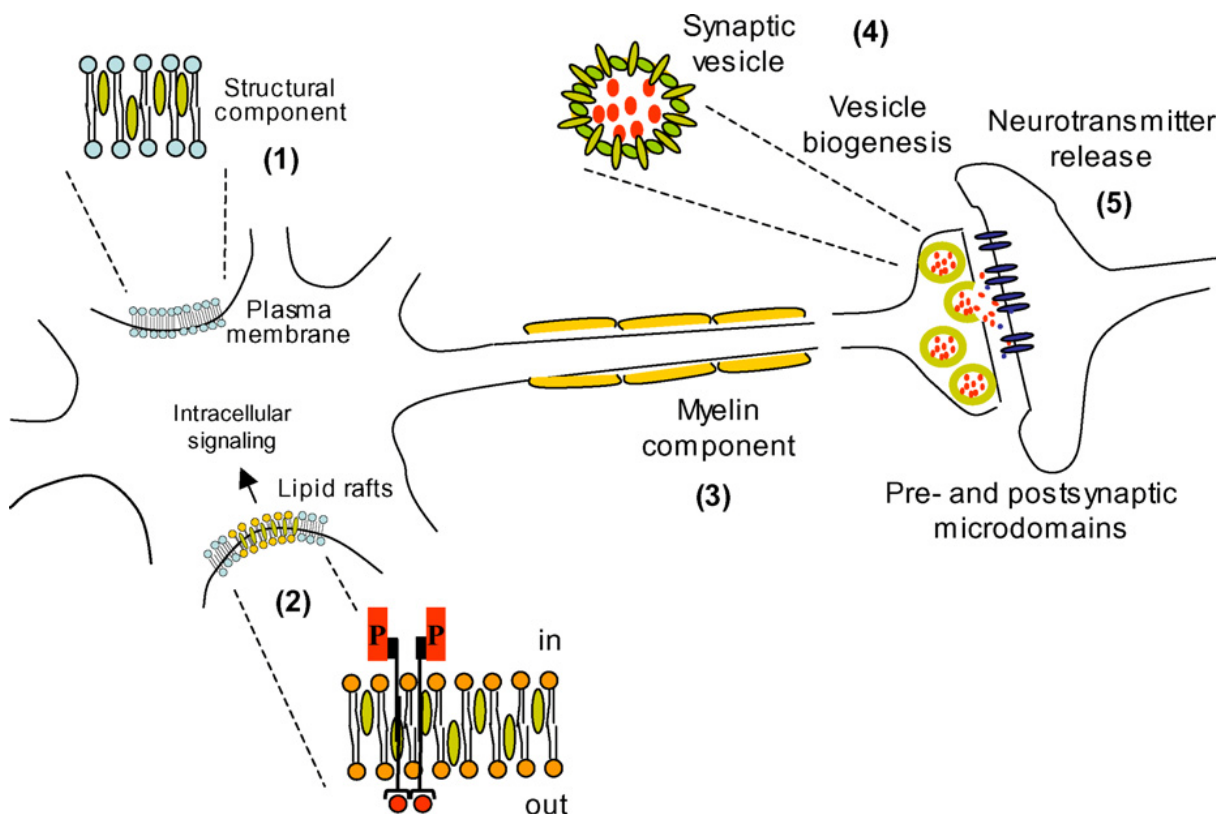


Fig. 1.5.: Cholesterol (green ovals) functions in neurons. Cholesterol is the major structural component of membranes (1), and it is also concentrated in micro domains (or lipid rafts) in plasma membranes in order to organize the signal transduction events triggered by different neurotrophic factors and their receptors (2). Up to 70% of brain cholesterol is associated with myelin (yellow) (3). Finally, cholesterol plays a crucial role during synaptogenesis (4) and optimal neurotransmitter release in pre- and post-micro domains (5) (Valenza, Cattaneo et al., 2006).

During brain maturation, and before astrocyte differentiation, neurons are able to cover their own cholesterol requirements through endogenous neo-synthesis (Valenza, Cattaneo et al, 2006).

In post-natal life this pathway is reduced significantly and neurons have to rely on the delivery of cholesterol from astrocytes through lipoproteins, such as ApoE (Mauch et al., 2001; Pfrieger, 2003).

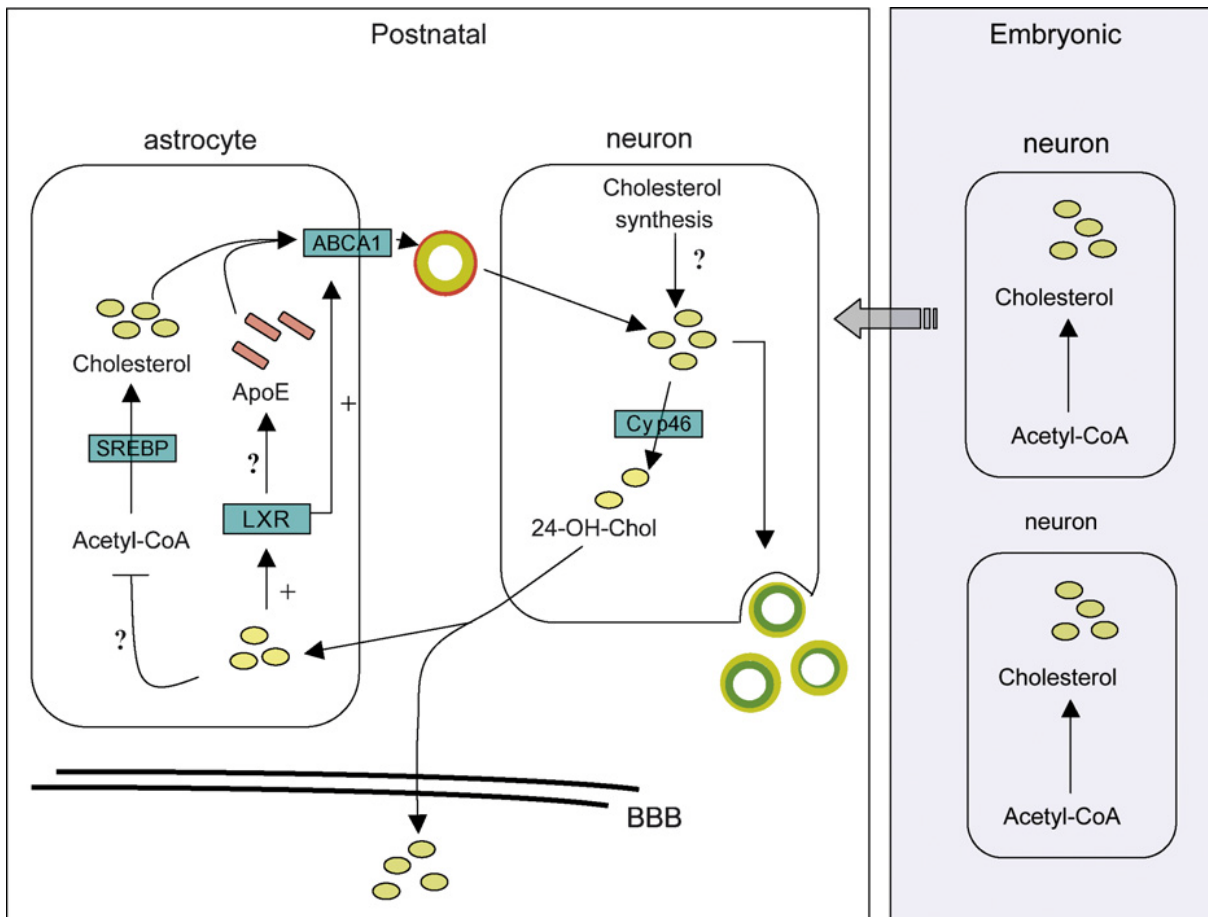


Fig. 1.6.: Hypothetical model of cholesterol homeostasis in neurons proposed by [Pfriege \(2003\)](#). During embryogenesis (right panel), neurons synthesize the cholesterol (green ovals) necessary for their requirements; after astrocyte differentiation and neuron maturation, neurons reduce this synthesis to a low basal level and import most cholesterol from astrocytes through apolipoproteins, such as ApoE (red rectangles). Cholesterol levels are regulated by the conversion of cholesterol to 24S-hydroxycholesterol (24-OH-Chol, yellow oval), which can cross the blood–brain barrier (BBB) more easily than cholesterol itself. This sterol is a potent activator of liver X receptors (LXRs), and may activate the efflux of cholesterol from astrocytes and inhibit cholesterol synthesis.

#### 1.4.1 Brain cholesterol in Huntington's disease

Recent studies of HD in mice and patients have suggested the possibility that it might also involve a defect in cholesterol homeostasis (Valenza, Cattaneo et al, 2006). Findings further revealed, that plasma levels of 24S-hydroxycholesterol (24OHC), the brain specific elimination product of cholesterol considered as a marker of brain cholesterol turnover, have been significantly reduced in HD patients at any disease stage (Leoni et al, 2011).

One important clinical feature of HD is a radical change in nutritional status (Trejo et al.,

2004), with weight loss being frequent. In consequence, greater body weight is associated with slower rate of disease progression (Myers *et al.*, 1991). The reasons for the dramatic weight loss are still unknown.

At later stages of HD, avitaminosis and other nutritional deficiencies have been reported as causes of death (Lanska *et al.*, 1988).

This is of relevance since cholesterol is the precursor of vitamin D and thus also steroid hormones like testosterone, which is reduced in plasma of HD male subjects (Markianos *et al.*, 2005), and bile acids.

Despite these clinical features, very little attention has been paid to these mechanisms and to the possibility that cholesterol may be involved in the manifestation of HD (Valenza, Cattaneo *et al.*, 2006).

This might have been because HD is a neurological disease and peripheral abnormalities were considered as being secondary events and/ or having less impact, although huntingtin is ubiquitously expressed and cholesterol is a key component of peripheral membranes and highly enriched in the brain (Valenza, Cattaneo *et al.*, 2006).

One first aspect to consider is that coenzyme Q10, which is synthesized from the intermediary metabolites of the cholesterol biosynthesis pathway, is used as a dietary supplement in many neurodegenerative diseases, including Parkinson's disease and HD, and that a diet enriched with fatty acids and ethyl-EPA reduces motor deficits in various HD mice strains (Clifford *et al.*, 2002; Van Raamsdonk *et al.*, 2005).

Recent data obtained from cells and tissue specimens of HD subjects, as well as molecular, biochemical and biological studies of HD mice and in vitro cell models, support the assumption that the cholesterol pathway is affected (Valenza, Cattaneo *et al.*, 2006).

Still further studies have to be made and also more epidemiological data has to be evaluated.

#### **1.4.2. In vitro or in vivo attempts for cholesterol rescue**

As alternative to de novo synthesis, cells can import cholesterol from an external source (Pfrieger et al, 2011). Nourishing cells secrete cholesterol as lipoproteins, which are taken up by target cells via specific receptors (Ikonen et al., 2008). If there are specific receptors for taking up cholesterol, there must be also a way to add cholesterol if it's pathologically reduced, like in HD.

The most promising approach to add cholesterol to the brain is the use of NPs with encapsulated cholesterol.

Still there are various problems like the interactions of the NPs with the reticulo endothelial system (RES), which rapidly eliminates NPs from circulation; moreover it is not clear if it is possible to localize the active component in a specific area of the CNS, which could be important for the treatment of chorea huntington.

## **2. Aim of the work**

The implementation of cholesterol, with the addition of exogenous cholesterol in the CNS appears as a feasible approach for the combined treatment of Huntington's disease. Unfortunately, the cholesterol does not pass the blood-brain barrier (BBB) in therapeutically relevant amounts. Considering the non-invasive approach, nanocarriers, and particularly polymeric nanoparticles could be employed to deliver exogenous cholesterol into the brain.

During my work different NPs were prepared with the aim to encapsulate as much cholesterol as possible.

It was tried to elaborate an optimized encapsulation process. This was done by changing several parameters of the working process and considering small differences of the prepared NPs.

After fine-tuning parameters and emerging the method with highest encapsulation efficiency of cholesterol, the next aim was to disclose the most appropriate additive for storage of frozen NPs and to resuspension.

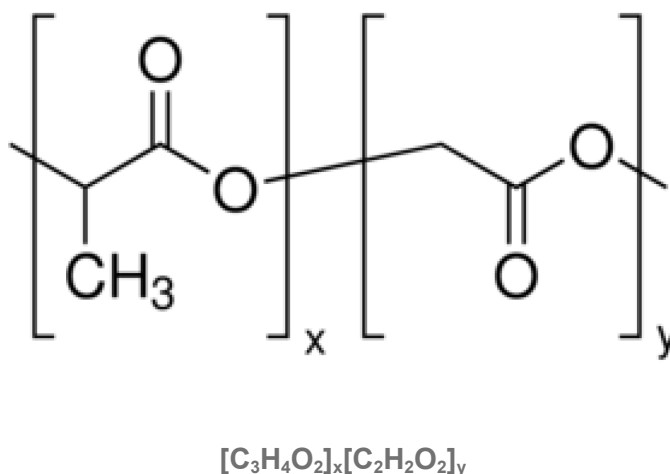
Finally, in an attempt to improve the release rate of cholesterol the impact of different kinds of sugar was investigated.



### 3. Materials

#### 1. Poly(lactic-co-glycolic acid)

##### PLGA



**Aspect:** white, amorphous and odorless powder

**Composition:** molar ratio between D,L lactic and glycolic acid between 48:52 and 52:48

**Solvents:** chlorinated solvents, tetrahydrofuran, acetone or ethyl acetate

PLGA is a copolymer of poly lactic acid (PLA) (x) and poly glycolic acid (PGA) (y) and is approved by the FDA for drug delivery due to biodegradability and biocompatibility.

In the experiments the non-H types of PLGA 503 and PLGA 502 referring to polymers with methylester end groups were used and purchased from Boehringer Ingelheim.

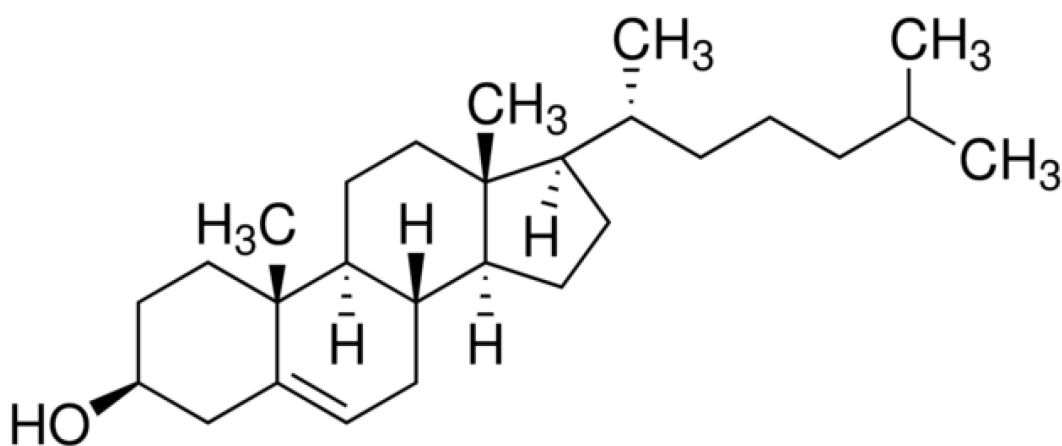
## PLGA RESOMER® RG 503

RESOMER® Type	Product Name	Molecular Weight Range	Viscosity (dl/g)	Application	Tg (°C)	Tm (°C)	End Group
RESOMER® RG 503	Poly(D,L-lactide- co-glycolide) 50:50	24000- 38000	0.32- 0.44	controlled release	44-48	amorphous	ester

## PLGA RESOMER® RG 502

RESOMER® Type	Product Name	Molecular Weight Range	Viscosity (dl/g)	Application	Tg (°C)	Tm (°C)	End Group
RESOMER® RG 502	Poly(D,L-lactide- co-glycolide) 50:50	7000- 17000	0.16- 0.24	controlled release	42-46	amorphous	alkyl ester

## 2. Cholesterol



**aspect:** white, amorphous powder, odorless

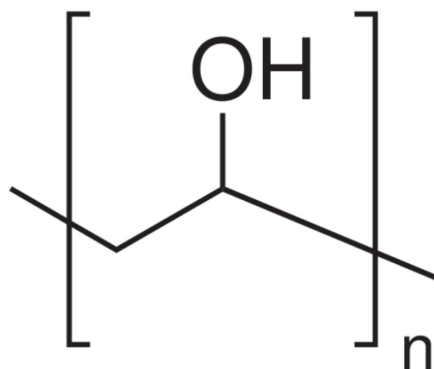
**characteristics:** insoluble in water (less than 0.5 mg/100 ml of water); slightly soluble in alcohol, ether, chloroform, pyridin, more soluble in hot alcohol; soluble in acetone, dioxane, ethyl acetate, benzene, petroleum ether, oils, fats, and in aqueous solutions of bile salts

**producer:** Sigma-Aldrich

chemical formula	C <sub>27</sub> H <sub>46</sub> O
molecular weight	386.7 Da

### 3. Polyvinyl alcohol

#### PVA



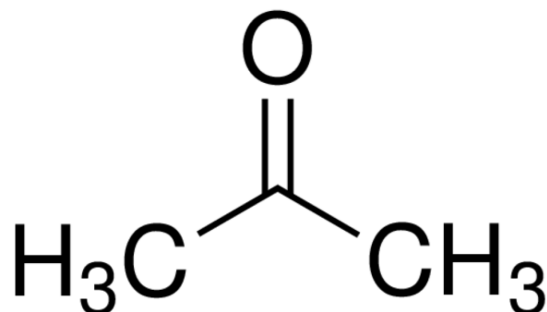
**characteristics:** powder, odorless, nontoxic, degradable, hydrophilic and water soluble, FDA approved for parenteral preparations

In the experiments PVA with the molecular weight of 15000 Da was used.

A 1% solution in water was prepared.

chemical formula	(C <sub>2</sub> H <sub>4</sub> O) <sub>x</sub>
molecular weight	15000 Da
density	1.19-1.31 g/cm <sup>3</sup>

#### 4. Acetone

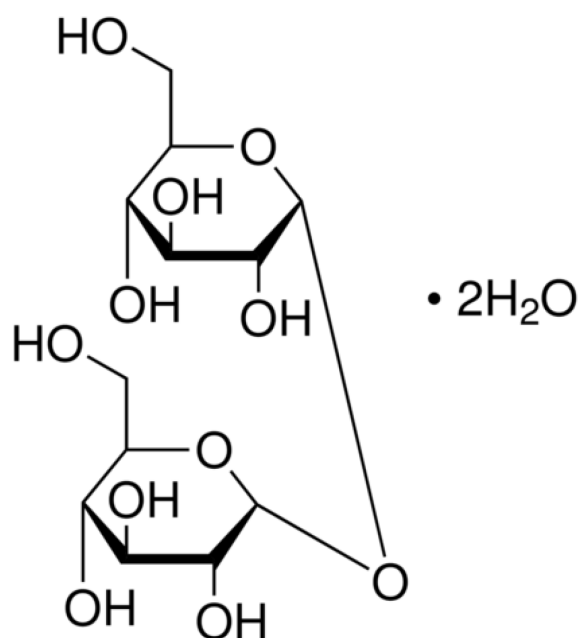


**characteristics:** colorless, inflammable, specific smell, miscible with water, ethanol and ether, toxic

**producer:** Sigma-Aldrich

chemical formula	C <sub>3</sub> H <sub>6</sub> O
molecular weight	58 Da

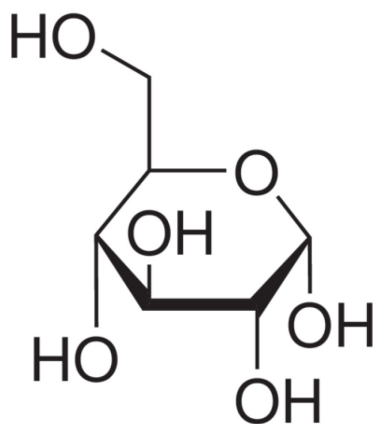
## 5. D-(+)-Trehalose dihydrate



**characteristics:** odorless, white powder, water soluble

chemical formula	<b>C<sub>12</sub>H<sub>22</sub>O<sub>11</sub> · 2H<sub>2</sub>O</b>
molecular weight	<b>378.33 Da</b>

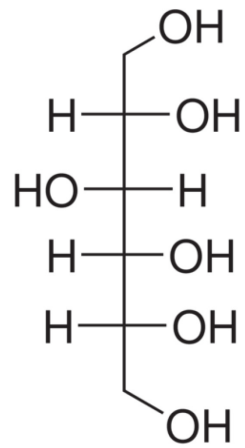
## 6. Glucose



**characteristics:** odorless, white powder, water soluble

chemical formula	<b>C<sub>6</sub>H<sub>12</sub>O<sub>6</sub></b>
molecular weight	<b>180.16 Da</b>

## 7. D-Sorbitol

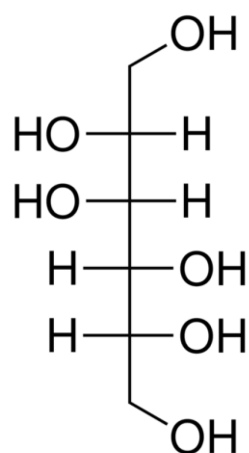


**characteristics:** odorless, white powder, water soluble

chemical formula	<b>C<sub>6</sub>H<sub>14</sub>O<sub>6</sub></b>
molecular weight	<b>182.17Da</b>



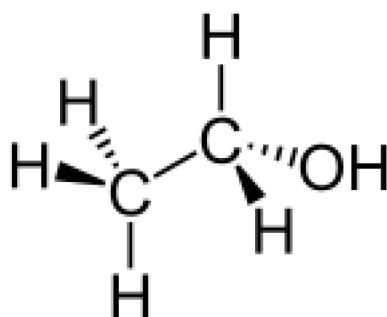
## 8. D-Mannitol



**characteristics:** odorless, white powder, water soluble

chemical formula	<b>C<sub>6</sub>H<sub>14</sub>O<sub>6</sub></b>
molecular weight	<b>182.17Da</b>

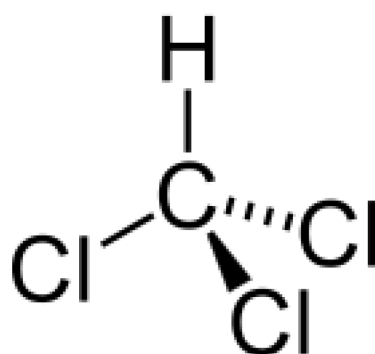
### 9. Ethanol, absolute



**characteristics:** clear, transparent liquid; strong characteristic odor; inflammable

chemical formula	CH <sub>3</sub> CH <sub>2</sub> OH
molecular weight	<b>46,1 Da</b>

## 10. Chloroform

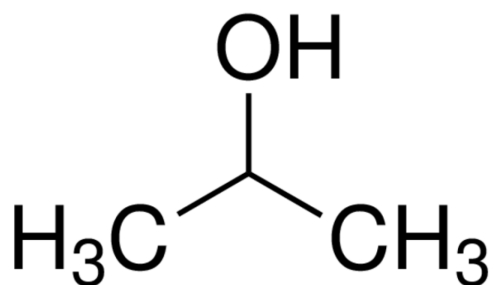


**characteristics:** clear, transparent liquid; strong sweet characteristic odor;  
inflammable

chemical formula	$\text{CHCl}_3$
molecular weight	<b>119.38 Da</b>

## 11. Isopropyl Alcohol

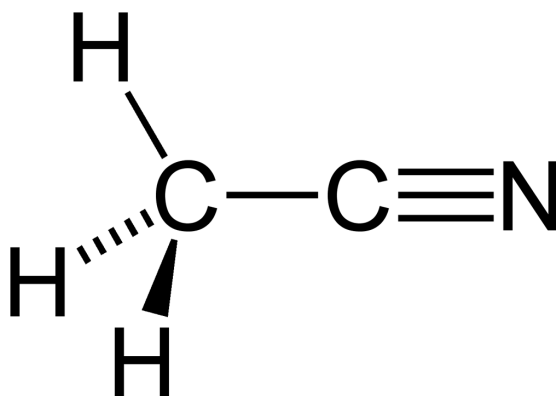
IPA



**characteristics:** clear, transparent liquid; inflammable

chemical formula	<b>(CH<sub>3</sub>)<sub>2</sub>CHOH</b>
molecular weight	<b>60.1Da</b>

## 12. Acetonitrile



**characteristics:** clear, transparent liquid; inflammable

chemical formula	CH <sub>3</sub> CN
molecular weight	<b>41.05Da</b>

## 4. Methods

### 4.1. Preparation of Np

Nanoparticles were prepared according to the nanoprecipitation method.

#### 4.1.1 Nanoprecipitation

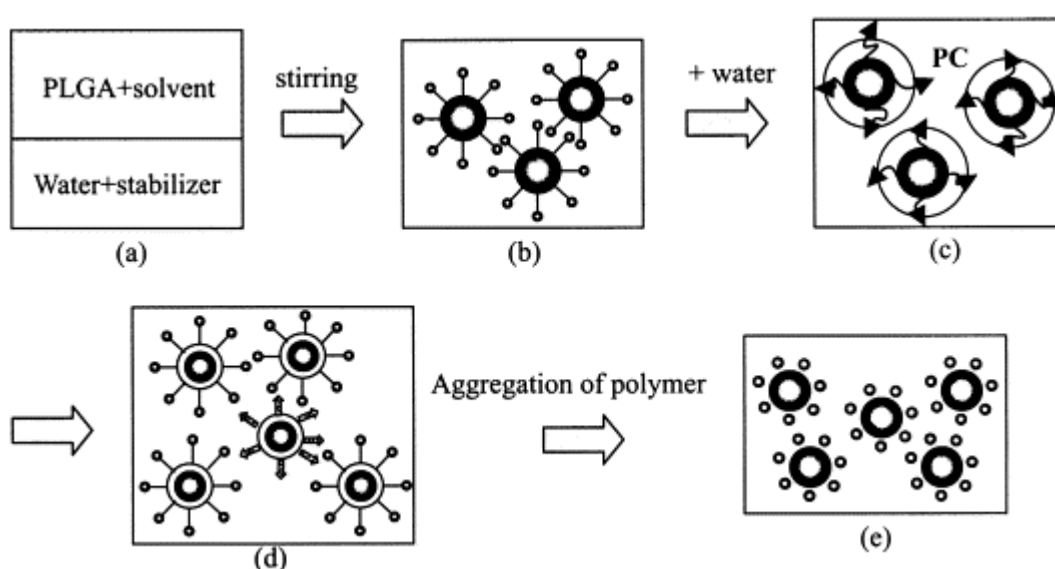


Fig. 4.1. Schematic description of formation of PLGA nanoparticles by the emulsification–diffusion method. *Adapted from: Preparation of PLGA nanoparticles containing estrogen by emulsification–diffusion method, Colloids and Surfaces A: Physicochemical and Engineering Aspects Volume 182, Issues 1–3, 30 June 2001, Pages 123–130.*

Approximately 50.0 mg of polymer (Resomer 503 or Resomer 502) and varying amounts of cholesterol were co-dissolved in 4 ml acetone. The organic phase was added dropwise to the aqueous phase (12,5 ml 1% aqueous PVA if not indicated otherwise) under stirring. When acetone is added to the aqueous phase it is mixed and the solubility of the PLGA in acetone/water-droplet is reduced leading to polymer precipitation and therefore to generation of nanoparticles (NPs). The presence of surfactant allowed the formation of small particles (100-200nm) and their stabilization during the formulation and processing.

When sugar was investigated as a release-promotingauxiliary agent, a saturated solution

in acetone was applied. For that purpose about 20 mg sugar and 10 ml acetone were stirred in a well-closed vial for at least 24 hours. For the experiments only the supernatant free of undissolved carbohydrate was used for dissolving the polymer and cholesterol as described above.

Finally, after nanoparticle formation, the solvent was completely removed by evaporation using a rotavapor (ROTAVAPOR-Buchi R 114) at 30°C for at least 20 minutes. When the solvent was completely removed nanoparticles were collected by ultracentrifugation.

#### **4.1.2. Purification and collection of the nanoparticles**

To remove the un-encapsulated Cholesterol and PVA from the NPs, all the samples were centrifuged after testing two different centrifugation rates (15000 and 17000 rpm, respectively) for 10 min (Sorvall RC28S, Dupont, Brussels, Belgium), washed with milliQwater and re-suspended in water. The purified NPs suspensions were freeze-dried (-60°C, 1.10<sup>-3</sup> mm/Hg, 48 hrs; LyoLab 3000, Heto-Holten, Allerød, Denmark) after addition of different amounts and types of cryoprotectors (PVA or trehalose). All the samples were stored at 4°C in dark.

### **4.2. Characterization of nanoparticles**

#### **4.2.1. Morphology of nanoparticles**

A scanning electron microscope (SEM) (XL-40 Philips, Eindhoven, The Netherlands) (× 10,000) was used to evaluate the morphology of NPs. Purified nanoparticles were diluted (about 0,5mg/ml) and few drops of the suspension were dried on a stub for at least 24 hours. The samples were sputter coated under argon atmosphere with gold palladium yielding a 10 nm film (Emitech K550 Supper Coated, Emitech LTD, U.K.).

#### 4.2.2 Size and zeta potential of nanoparticles

These characteristics were acquired by Photon Correlation Spectroscopy (PCS), using the Zetasizer Nano ZS (Malvern Instrument, UK; Laser 4 mW He–Ne, 633 nm, Laser attenuator Automatic, transmission 100–0.0003%, Detector Avalanche photodiode, Q.E. > 50% at 633 nm, T = 25°C). Applying this technique both, dimension (expressed as Z-Average, PDI ) and zeta-potential were determined.

This technique is based on the principle that dispersed particles move randomly in all spatial dimensions, the so-called Brownian motion. There is a relationship between Brownian motion and particle size: large particles move slowly, while small particles move quickly. These motions can be described in a quantitative way by the Stokes-Einstein equation by determination of the translational diffusion coefficient (D), which is inversely proportional to the diameter of the particle (d):

$$d(H) = \frac{KT}{3\pi\eta D}$$

where

- K is the Boltzmann's constant
- T is the absolute temperature
- $\eta$  is the viscosity
- D is the diffusion constant
- d(H) is the hydrodynamic diameter or Stokes' diameter, means the diameter of the particle including its solvent shell

The coefficient D of the particles is acquired by the instrument on the basis of the intensity of light scattered by the suspension. When a light beam, generally a laser, crosses the suspension part of the photons that pass through it is scattered 3-dimensionally, giving rise to a certain speckle pattern. For a system undergoing Brownian motion, the intensity of the speckle pattern fluctuates by time: Small particles move quickly and rapid fluctuations in intensity are observed, while large particles move slow resulting in low intensity



fluctuations of the speckle pattern. In order to collect these events changing in the msec-range, a correlation function is used for calculation of the translational diffusion coefficient, which is the basis for calculation of the hydrodynamic diameter according to the Stokes-Einstein equation. Using mathematical methods is also possible to decompose the autocorrelation function so as to identify the different populations dimensional sample.

For the measurement the suspension was diluted 1:100 and about 500  $\mu\text{l}$  were put in a plastic low volume sizing cuvette.

#### **4.2.3. Zeta-Potential measurement**

Even the surface charge is of considerable importance for the characterization of particulate systems. When a particle dispersed in a liquid, generally it is surrounded by ions present in the medium that are attracted by electrostatic interactions. This distribution results in an increase of the concentration of counter ions (ions of opposite charge to that of the particle). In particular, the layer of liquid with the ions surrounding the particle is composed of two areas: one internal (stationary layer) with ions strongly bound to the charged particle, and an outer (diffuse) layer where interactions are weakened due to distance.

Since the intrinsic charge on the particle surface is shielded from the charges of the stationary layer, the interactions between particles will obviously be precisely guided by the potential present at the surface of this layer. Within the diffuse layer there a so-called slipping plane representing the boundary between fluid layer remaining attached to the particle upon shear due to Brownian movement and the fluid layer that is slipped off. The potential at this plane is called zeta potential.

Since in an electrical field the movement of particles towards the oppositely charged electrode is depends on surface charge, the electrophoretic mobility of the particles is the key issue for determination of the zeta potential.

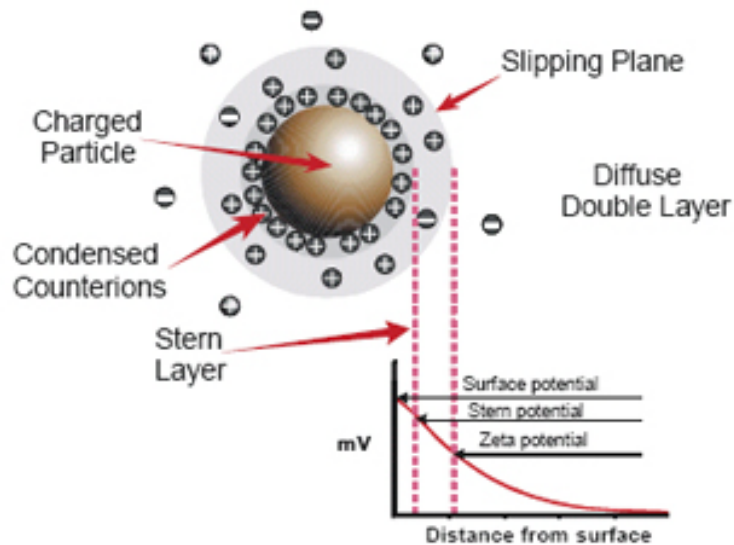


Fig.4.2. Scheme of the distribution of ions around a charged particle, picture taken from pharmaceuticalonline.

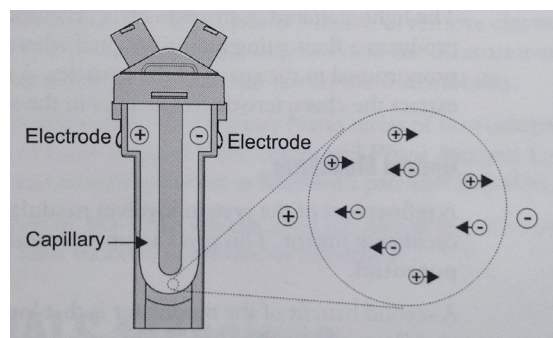


Fig. 4.3. Scheme of the capillary cell. Picture taken from interdepartmental equipment facility (Malvern Instructions for zeta sizer).

The velocity of the movement depends on the intensity of the electric field, the dielectric constant of the medium (here water), the viscosity of the medium and the Zeta potential. The velocity is called electrophoretic mobility, expressed by the Henry equation:

$$U_E = \frac{2\epsilon\zeta F(\kappa a)}{3\eta},$$

where:

- $U_E$  is electrophoretic mobility

- $\epsilon$  is the dielectric constant
- $\zeta$  is the zeta potential
- $F(\kappa a)$  is the Henry function
- $\eta$  is the viscosity

$F(\kappa a)$  is 1,5 in aqueous media according to the Smoluchowski-approximation.

For the evaluation of the surface charge, 20  $\mu$ l of the suspension were diluted in 1ml distilled water. 750  $\mu$ L of the suspension were used for measurement in a microcell at 25 °C.

#### **4.2.4. Reconstitution of lyophilized nanoparticles**

The freeze dried NPs either pure or in presence of cryoprotectors were resuspended in MilliQwater. Briefly, 1mg lyophilized powder was sonicated (sonicator bath) in 1.0 ml water for 60 seconds. The grade of resuspension was estimated by size and zeta -potential. In case of polydisperse agglomerated samples a second sonication step was performed.

#### **4.2.5. Determination of entrapment efficiency**

##### **Extraction of cholesterol from nanoparticles:**

In order to correctly quantify the amount of cholesterol loaded into nanoparticles an extraction method had to be developed. For that purpose, about 5.00 mg NPs were dissolved in 0.5ml chloroform and 1.0 ml isopropyl alcohol. Since cholesterol is soluble in isopropyl alcohol, but PLGA is insoluble, the cholesterol accumulates in alcohol, while PLGA remains dissolved in trichlorethane or precipitates in the mixture. The mixture was shaken (Vortex 15 Hz) to promote the precipitation of PLGA. After removal of precipitated PLGA by filtering through a filter with 0.20  $\mu$ m pore diameter (PTFE, suitable for organic

solvent), the cholesterol solution was analyzed by HPLC. At least three samples were analyzed for each preparation lot.

### Quantification of cholesterol by HPLC

The cholesterol content of the samples was determined by High-performance liquid chromatography (HPLC) in combination with an UV detector. The instruments used were: HPLC-system Jasco PU 980, column Thermo scientific, Syncronics C18, 25cm x 4.6 mm and the detector Jasco UV 975.



Fig. 4.4. Detector Jasco UV 975.



Fig 4.5. HPLC system Jasco PU 980.



Fig. 4.6. Column thermo scientific, Syncronics C18, 25cm x 4.6 mm.

HPLC consists of a column with the stationary phase for the separation, a pump that moves the mobile phase with the sample through the column with high pressure and a

detector that detects the substance and records substance-characteristic retention times, which means the time that the compound needs to pass the column, and signals expressed by areas that depend on the amount of each component. The wavelength of the UV detector was set at 240 nm.

The retention times are specific for each compound caused by the different chemical or physical interaction with the column. For the experiments HPLC-grade chemicals were used.

There are two modes of eluting the compounds from the column, isocratic or gradient elution. In case of isocratic elution the composition of the mobile phase is kept constant over time, like in our experiments, whereas gradient elution means that the composition of the mobile phase is varied during the measurement. The mobile phase we used was acetonitrile/ethanol (1+1, V/V).

Not only the exact composition of the mobile phase is important for reproduce able results but also the pressure and the flow and the sample volume. A constant flow was ensured by a pump in the ranging from 0.1 to 10 ml/min and was set at 1.2 ml/min.

The sample volume can vary between 5 $\mu$ l and 500  $\mu$ l and is set firstly with a syringe and secondly with a loop. In our experiments a loop with 50 $\mu$ l sample volume was applied.



Fig. 4.7. Syringe used for injections.



Fig. 4.8. Sample loop with 50  $\mu$ l volume.

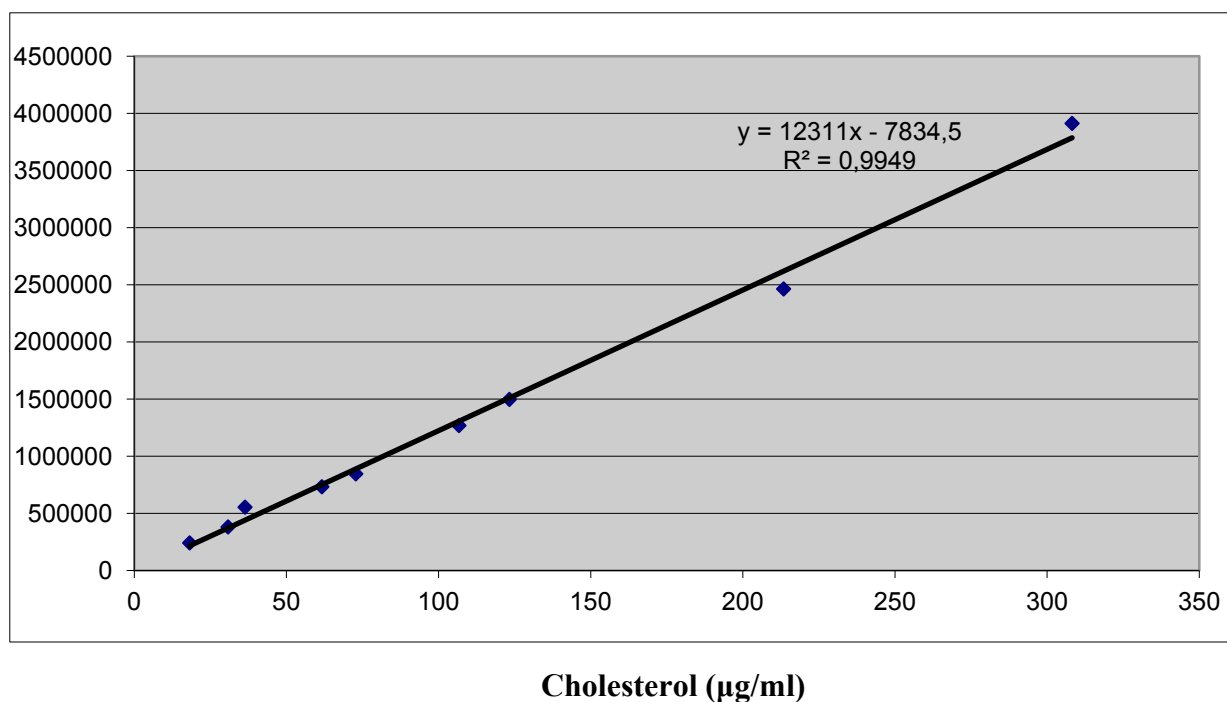
To exactly quantify the amount of cholesterol loaded into nanoparticles a calibration curve was acquired analyzing a series of dilutions of cholesterol in chloroform/isopropyl alcohol (1+2, V/V).

The calibration graph was characterized by:

$$y = 12311x - 7834.5$$

$$R^2 = 0.9949$$

### Area



## 5. Results

### 5.1. Characterization of cholesterol-loaded Resomer® 503- Nps

Cholesterol loaded PLGA nanoparticles were prepared according to the nanoprecipitation-technique (as described in the methods section), and optimized in the laboratory of TeFarTi (Modena) group as reported below.

<b>Surfactant</b>	<b>PVA1%</b>
<b>Organic solvent</b>	<b>acetone</b>
<b>Polymer concentration in organic phase</b>	<b>12.5 mg/ml</b>
<b>Water /organic solvent ratio</b>	<b>3.12</b>

Table 5.1. General parameter settings for preparation of cholesterol-loaded Resomer®503- Nps.

In this study, PLGA Resomer® 503 characterized by molecular weight range between 24000 and 38000 was used and some formulation parameters such as the ratio between polymer and drug (cholesterol, Chol) and the purification method (as reported in table 5.2) have been investigated.

<b>Sample</b>	<b>Polymer</b>	<b>mg Cho/100 mg PLGA</b>	<b>Chol-PLGA weight ratio</b>	<b>Purification</b>
<b>chol 1a</b>	RESOMER®503	1	1:100	17000 rpm 10 min
<b>chol 1b</b>	RESOMER®503	1	1:100	15000 rpm 10 min
<b>chol 2a</b>	RESOMER®503	5	1:20	17000 rpm 10 min
<b>chol 2b</b>	RESOMER®503	5	1:20	15000 rpm 10 min
<b>chol 3a</b>	RESOMER®503	10	1:10	17000 rpm 10 min
<b>chol 3b</b>	RESOMER®503	10	1:10	15000 rpm 10 min

Table 5.2. Variation and cholesterol/PLGA-ratio and centrifugation settings during preparation and characterization of cholesterol-loaded Resomer®503- Nps.

All the formulations were prepared from 50 mg polymer since previous data have demonstrated that Nps can be prepared from higher amounts of polymer (at least up to 150mg) by simply adapting the volume of organic and water phase. For simplicity, in table 5.2., data related to 100 mg polymer are reported.

After preparation the nanoparticles samples were purified using ultracentrifugation technique at 17000 rpm (*chol 1a, chol 2a and chol 3a*) or 15000 rpm (*chol 1b, chol 2b and chol 3 b*) for 10 minutes.

#### **5.1.1 Physico-chemical characterization of cholesterol-loaded Resomer<sup>®</sup> 503- Nps**

All the formulations were characterized by measuring the size and the Zeta Potential (Z-Potential) by Photon Correlation Spectroscopy technique.

Nanoparticles hydrodynamic diameters were expressed as Zeta- Average (Z-Average), which represents the mean of the single determinations. Moreover, D10, D50 and D90 were recorded to assess the value of the size below, which the 10% [D (10)], 50% [D (50)] and 90% [D (90)] of all the samples is present. Simultaneously, the polydispersity index (PDI) expressing the homogeneity of the sample was acquired.

For each preparation, the measurements were performed immediately after formulation (before centrifugation, pre centr) and after the purification process (post centr).



### Pre centrifugation:

Name	Z average ± SD (nm)	PDI	D10 (nm)	D50 (nm)	D90 (nm)	Z-potential (mV)	Z -deviation
empty	175± 12	0.07	118	176	265	-7.6	4.5
chol 1 a	178 ±11	0.08	120	182	278	-6.0	9.3
chol 1 b	160 ± 13	0.11	111	166	254	-7.4	8.4
chol 2 a	158 ±12	0.11	102	160	259	-7.1	13.6
chol 2 b	179 ±10	0.08	128	186	275	-12.1	12.9
chol 3 a	166 ±13	0.15	114	169	251	-27.1	37.1
chol 3 b	174 ± 9	0.10	117	184	294	-12.5	7.6

Table 5.3. Size and zeta-potential of cholesterol-loaded Resomer®503-Nps immediately after preparation.

As the diameter of all the formulations was between 160 nm and 180 nm and no significant differences were observed, variation of the amount of added cholesterol did not affect the size of the Nps.

The PDI values were in the range of 0.08 - 0.15. Generally, values lower than 0.1 indicate a monomodal and highly homogenous size distribution. According to the data in Tab. 5.3. all the Nps are nearly monomodal and monodisperse, which is as also confirmed by the D10, D50, and D90-values that show small variation from 100 nm to 290 nm.

As the Nps were prepared from end-capped PLGA which mainly contains only a terminal hydroxyl-group and no free carboxyl-groups the Nps formulations exhibited a slightly Zeta-Potential. Whereas the zeta-potential of Nps prepared with 1% and 5% Chol was comparable, increasing the added amount of Cholesterol to 10% resulted in a markedly increase in negative surface charge of the Nps.

## Post centrifugation:

Name	Z average ± SD (nm)	PDI	D10 (nm)	D50 (nm)	D90 (nm)	Z-potential (mV)	Z-deviation
empty	181 ± 9	0.08	139	187	175	-11.7	6.7
chol 1 a	192 ± 10	0.09	136	195	283	-9.1	9.0
chol 1 b	165 ±8	0.07	118	172	252	-8.4	11.9
chol 2 a	176 ± 11	0.11	118	177	269	-16.3	17.9
chol 2 b	180± 8	0.06	128	186	274	-17.2	8.3
chol 3 a	161 ± 9	0.08	111	168	257	-7.0	9.8
chol 3 b	182 ±10	0.09	126	189	291	-11.4	6.2

Table 5.4. Size and zeta-potential of cholesterol-loaded Resomer®503- Nps after purification

After centrifugation at 15000 or 17000 rpm, respectively, for 10 minutes the supernatant was removed and the Nps pellet was re-suspended in water in a sonication bath for 1 - 2 minutes. As all parameters collected, the zeta-potential, the hydrodynamic diameter, and the PDI were similar to that prior centrifugation; removal of impurities and by-products by centrifugation is most appropriate. Moreover, since resuspension of the particles by short incubation in a sonication bath underlined redispersibility of the Nps.

All the formulations were also characterized by high yield amounting to  $41 \pm 8$  mg of formulation corresponding to an efficiency of 82%, which was calculated by simply weighing the lyophilized pellet.

### 5.1.2 Morphological characterization of 5 cholesterol-loaded Resomer®503- Nps

Purified nanoparticles were morphologically characterized by scanning electron microscopy (SEM).

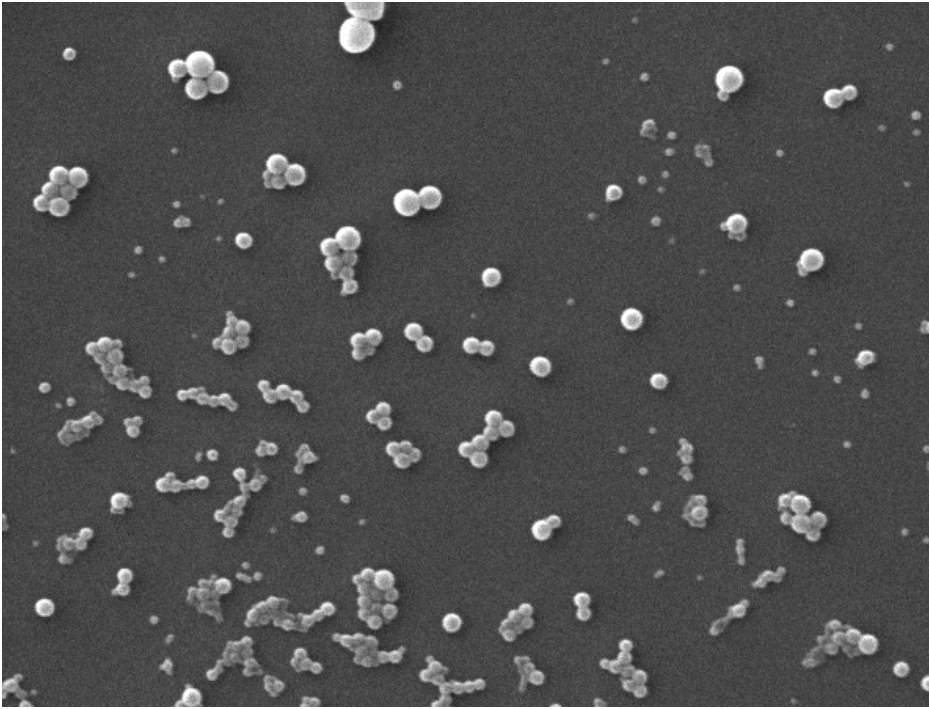


Fig. 5.5.: SEM image of cholesterol-loaded Resomer®503- Nps prepared at a chol/PLGA ratio of 1:100. Magnification, 15.000x.

The nanoparticles possess a clearly round, spherical shape, being either well separated or with some agglomerates due to the low Tg of PLGA.

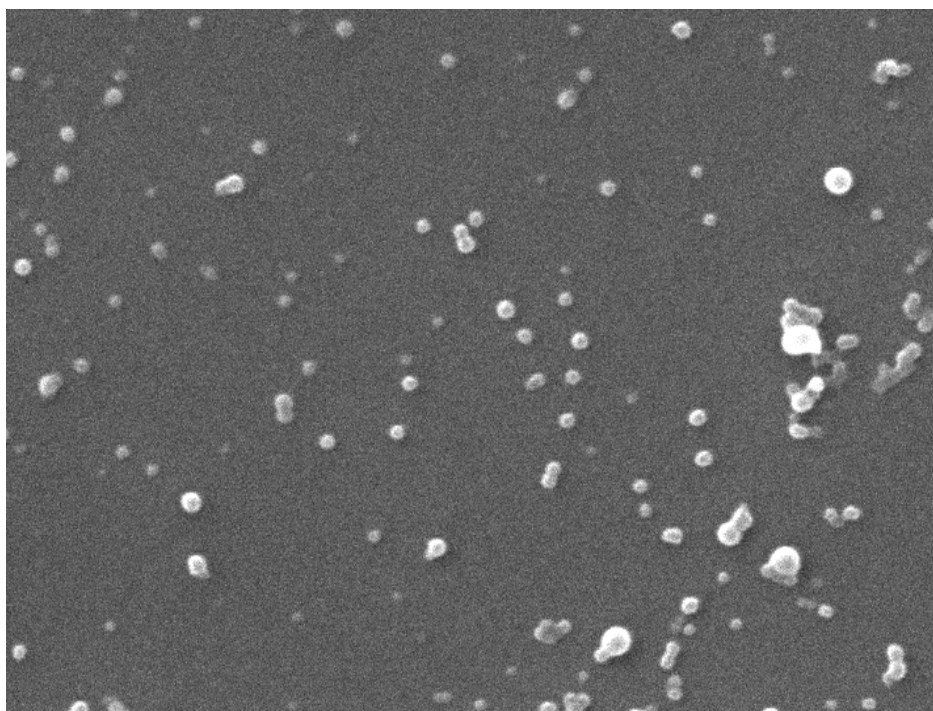


Fig 5.6.: SEM image of cholesterol-loaded Resomer®503- Nps prepared at a chol/PLGA ratio of 1:20. Magnification, 15.000x.

SEM image of Chol2b, reported in figure 5.6 showed well formed and spherical Nps. Few clusters of two Nps were visible.

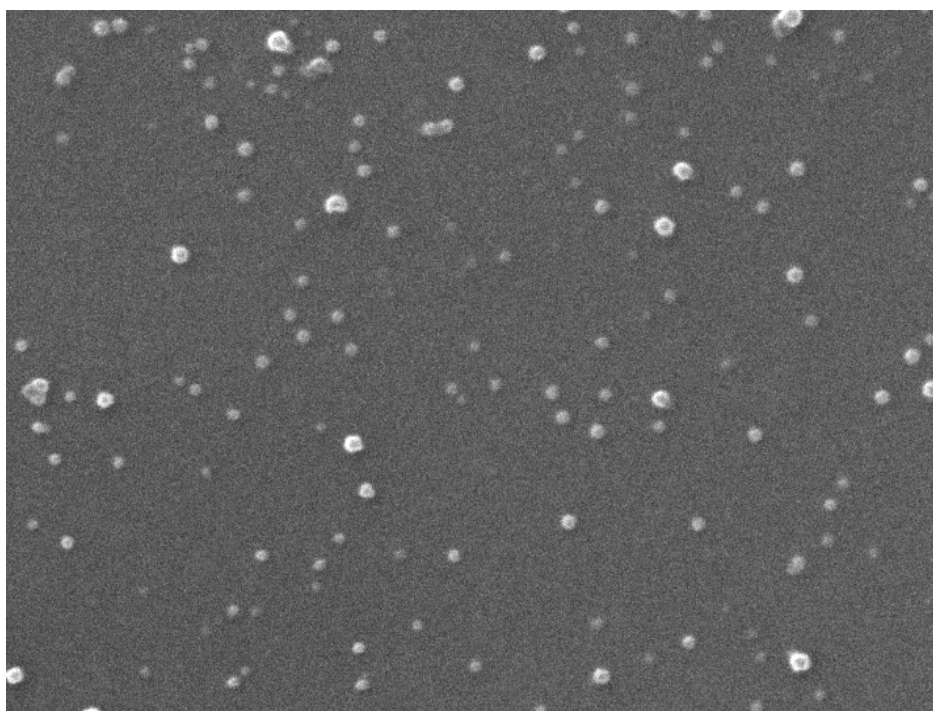


Fig. 5.7.: SEM image of cholesterol-loaded Resomer®503- Nps prepared at a chol/PLGA ratio of 1:10. Magnification, 15.000x.

Finally, in figure 5.7. chol 3a appears as defined and spherical nanoparticles, without any aggregates most probably due to high dilution of the sample.

### **5.1.3 Encapsulation efficiency of cholesterol-loaded Resomer®503- Nps**

To determine the amount of entrapped cholesterol the purified samples were freeze-dried and a defined amount of powder was used to extract the cholesterol and followed by quantitation by HPLC.

Sample	theoretical content (mg chol/100 mg formulation)	Practical content (mg Chol/100 mg formulation)	ENCAPSULATION EFFICIENCY (%)
chol 1a	1	0.70 ( $\pm 0.10$ )	68.7 ( $\pm 7.4$ )
chol 1b	1	0.67 ( $\pm 0.03$ )	65.8 ( $\pm 4.5$ )
chol 2a	5	0.93 ( $\pm 0.03$ )	18.6 ( $\pm 0.6$ )
chol 2b	5	1.28 ( $\pm 0.07$ )	25.7 ( $\pm 0.3$ )
chol 3a	10	2.38 ( $\pm 0.03$ )	23.8 ( $\pm 3,4$ )
chol 3b	10	2.09 ( $\pm 0.06$ )	20.9 ( $\pm 0.4$ )

Table 5.8. Encapsulation efficiency of cholesterol-loaded Resomer®503-Nps.

According to the data in Table 5.8. NPs prepared from 1 mg cholesterol per 100 mg of PLGA stably incorporate about 0.7 mg of cholesterol, corresponding to 67% E.E.

Increasing the amount of cholesterol added leads to a quite linear increase of the total amount of entrapped cholesterol from about 1% (chol 2ab) to 2% (chol 3ab). Although the tenfold amount of chol was applied for preparation of chol 3 Nps, a fifth of the drug was incorporated in the Nps. Interestingly; again the entrapment efficiency was not influenced by the centrifugation speed during purification.

#### **5.1.4 Influence of type and amount of cryoprotectant on cholesterol-loaded Resomer®503- Nps**

In order to ensure the stability of the nanoparticulate drug delivery systems, the formulations were subjected to lyophilization in the presence of two cryoprotectants, trehalose or PVA.

To allow for long term storage of nanoparticles loaded with cholesterol, the influence of adding substances able to protect Nps during the freezing and the lyophilization process from agglomeration, thus making the formulation easily redispersible. Briefly, different amounts of PVA or trehalose were added before freezing and afterwards 1.0 mg of lyophilized powder was re-suspended in water by sonication in a bath for 2 minutes at the most. Then Z-Average, PDI, D10, D5, D90 and zeta-potential were recorded.

In absence of cryoprotectants, the lyophilized samples appeared to be poorly re-dispersible as characterized by large aggregates, which, even if subjected to sonication (120"), tended not to disaggregate.

The addition of trehalose at a weight ratio of 1:1 or 1:0.5 (polymer/trehalose, w/w) was sufficient to obtain well redispersible - systems. Upon further reducing the concentration of trehalose to 1:0.25 (w/w, polymer/trehalose), only the formulation prepared from 5 mg of Chol revealed sufficient results in terms of lack of aggregates and redispersibility.

In case of PVA, the samples were well redispersible upon addition of the cryoprotectant down to the ratios of 1:0.25 (w/w, PLGA/PVA). The addition of lower amounts of PVA 1:0,1 (w/w, PLGA/PVA) yielded results of lowest reproducibility and only the formulation prepared from larger quantities of cholesterol gave good results.

The zeta-potential of all formulations was negative and comparable to the data previously described for post centrifugation samples. Thus the electrostatic interactions between the particles have not been influenced by the lyoprotectants.

mg Chol/100 mg PLGA	cryoprotectant	PLGA-cryoprotectants (w/w)	Z-Average [nm] ± SD	PDI	D10 [nm]	D50 [nm]	D90 [nm]	Z-Potential [mV]	sonication time (seconds)
1	water	no	365 ± 54	0.45	171	356	2186	-8.5 (± 2.7)	120
5	water	no	573 ± 80	0.66	147	568	825	-3.1 (± 2.9)	120
1	threalose	1-1	218 ± 13	0.14	146	218	342	-11.6 (± 6.1)	60
1	threalose	1-0.5	200 ± 11	0.16	124	203	357	-7.47 (± 0.6)	60'
1	threalose	1-0.25	245 ± 23	0.27	141	231	1420	-9.2 (± 0.4)	60
5	threalose	1-1	183 ± 10	0.10	122	186	286	-13.5 (± 5.2)	60
5	threalose	1-0.5	178 ± 9	0.12	106	179	309	-8.7 (± 1.6)	60
5	threalose	1-0.25	185 ± 12	0.15	115	185	311	-12.9 (± 1.3)	60
1	PVA	1-2.5	202 ± 11	0.07	146	209	303	-11.7 (± 4.7)	60'
1	PVA	1-0.75	244 ± 18	0.27	172	291	315	-14.1 (± 1.1)	60'
1	PVA	1-0.25	213 ± 23	0.18	128	222	452	-8.1 (± 0.8)	120
1	PVA	1-0.1	265 ± 31	0.33	139	514	3290	-7.5 (± 0.3)	120
5	PVA	1-0.75	186 ± 9	0.05	126	190	286	-12.8 (± 1.7)	60
5	PVA	1-0.25	174 ± 8	0.09	113	174	272	-13.3 (± 1.4)	60
5	PVA	1-0.1	188 ± 11	0.14	120	186	293	-9.7 (± 3.4)	60

Table 5.9. Influence of cryoprotectants on size and zeta-potential of cholesterol-loaded Resomer®503- Nps.



## **5.2. Strategies to improve the cholesterol release from cholesterol-loaded Resomer®503- Nps**

Considering the high molecular weight and hydrophobicity of PLGA together with the low water solubility of cholesterol, the entrapped cholesterol is released most likely in the range between one and four weeks at the best. Consequently some approaches were followed to accelerate the release rate by co-entrapping hydrophilic compounds.

### **5.2.1. Addition of sucrose during matrix formation**

Firstly, Nps were made from Resomer® 503, as described in the previous chapter, in presence of a low molecular weight and highly hydrophilic molecule during the nanoprecipitation process. The rationale was that the hydrophilic molecule after dissolution in the organic phase is entrapped in the PLGA-matrix. Upon contact with aqueous media, this molecule acts as a “pore former” as it easily dissolves in water generating small channels for facilitated drug diffusion.

Due to their low molecular weight and high water solubility sugars were in the focus of interest. At the first sight, carbohydrates are most appropriate since they should be soluble in acetone, the solvent used during the nanoprecipitation, and then they should be able to partition fast into the aqueous phase.

As a basis for this approach, the saturation solubility of different carbohydrates in acetone was determined. For that purpose about 1 g of mannitol, trehalose, glucose or sorbitol was dispersed in 10 ml of acetone and magnetically stirred for at least 48 hours in a tightly closed vial. After centrifugation at room temperature 2.0 -3.0 ml of the supernatant was transferred into a crystallization vial and dried first at room temperature and finally in a dryer to remove residual solvent or humidity. Finally, the dried residues were accurately weighed and the saturation solubility of the different sugars in acetone was calculated.

<b>Sugar</b>	<b>solubility in acetone (µg/ml)</b>	<b>Temperature</b>
Mannitol	0.43	25°C
Trehalose	91.26	25°C
Glucose	200	25°C
Sorbitol	433	25°C

Table 5.10 . Saturation solubility of different sugars in acetone at room temperature.

In agreement with the literature [Arcos et al., 1998] mannitol was found to be very poorly soluble in acetone. The solubility of trehalose was about 210fold higher and that of glucose about 460fold. The highest solubility was observed in case of sorbitol being about 1000fold more soluble than mannitol.

Considering these results both, glucose and sorbitol were used to prepare sugar-modified nanoparticles.

### 5.2.2. Formulation and physico-chemical characterization of sugar-modified cholesterol-loaded Resomer® 503 Nps

Since the cholesterol/PLGA ratio of 1:100 yielded the highest encapsulation efficiency, this protocol was applied for investigation of the effect of carbohydrate-modification of PLGA-Nps.

<b>Sample</b>	<b>Chol-PLGA weight ratio</b>	<b>Sugar</b>	<b>saturated organic phase (mg)</b>	<b>Sugar in aqueous phase (g)</b>	<b>Purification</b>
<b>chol 4</b>	1:100	sorbitol	1.7		17000 rpm 10 min
<b>chol 5</b>	1:100	sorbitol	1.7	4	17000 rpm 10 min
<b>chol 6</b>	1:100	glucose	0.8		17000 rpm 10 min
<b>chol 7</b>	1:100	glucose	0.8	1.1	17000 rpm 10 min

Table 5.11. Preparation parameters of sugar-modified cholesterol-loaded Resomer® 503 Nps. Saturated organic phase refers to the amount carbohydrate dissolved in acetone and sugar in aqueous phase refers to the amount of carbohydrate dissolved in the aqueous layer.

According to table 5.11., the batch *chol 4* was prepared applying 4 ml sorbitol-saturated organic phase corresponding to a total amount of 1.7 mg sorbitol, while in batch *chol 5* both, the organic and the aqueous phase contained sorbitol. Whereas the organic phase was saturated, the aqueous phase contained 320 mg sorbitol/ml corresponding to 13.6% of its saturation solubility in water (2350 mg/ml). That way the diffusion of sorbitol from the organic to the aqueous phase is guaranteed due its high aqueous solubility and the presence of sugar-alcohol also in the PVA solution could permit further adsorption of sorbitol at the surface thus generating an irregular surface suitable for diffusion of cholesterol from the superficial layer of nanoparticles to the surrounding medium. Using glucose instead of sorbitol, the batches *chol 6* and *chol 7* were prepared analogously. For comparison, the aqueous PVA-solution contained 88 mg glucose/ml corresponding to 9.7% of the saturation solubility of glucose in water (910 mg/ml).

### Pre centrifugation

Sample	Z-Average ± SD (nm)	PDI	D10 (nm)	D50 (nm)	D90 (nm)	Zeta Potential (mV)	Z- Deviation
<b>chol 4</b>	163 ± 9	0.06	107	161	246	-8.9	8.1
<b>chol 5</b>	173 ± 5	0.06	121	176	255	-0.9	15.2
<b>chol 6</b>	156 ± 9	0.08	108	162	247	-6.0	9.7
<b>chol 7</b>	510 ± 11	0.09	450	530	785	-1.3	6.7

Table 5.12. Characteristics of sugar-modified cholesterol-loaded Resomer® 503 Nps immediately after preparation.

According to the results summarized in table 5.12 the size distribution of all Nps was monomodal and the size about 170 nm. In case of the batch prepared with glucose present in both layers (*chol 7*), however, the hydrodynamic diameter steeply increased to about 500nm. Since the glucose was present also in the aqueous phase and the diameter of a glucose molecule is only about 1nm it is supposed that adsorption of glucose might contribute to the increased diameter beside other still unknown effects.

Interestingly, the mean of the zeta-potential, although not significant, was dependent on the presence of glucose in the aqueous phase. Probably this effect observed is partly due to glucose adsorbed to the surface of the nanoparticles, which partly shields the negative charge of the hydrated particle. In addition, also a slightly higher viscosity of the sample

provoked by presence of high levels of glucose reduces electrophoretic mobility and thus the zeta-potential.

### Post centrifugation

Sample	Z <sub>average</sub> ± SD (nm)	PDI	D10 (nm)	D50 (nm)	D90 (nm)	Z potential (mV)	Z deviation
chol 4	173 ± 5	0.05	120	176	255	-10.5	7.8
chol 5	172 ± 8	0.06	129	197	306	-16.4	7.4
chol 6	167 ± 9	0.07	119	174	255	-5.7	9.9
chol7	161 ± 12	0.10	121	186	279	-27	5.3

Table 5.13. Characteristics of sugar-modified cholesterol-loaded Resomer® 503 Nps immediately after purification.

After the centrifugation at 17000 rpm for 10 minutes, all Np-batches demonstrated sufficient redispersibility after sonication for 1 minute. For the entire sample, the Z-Average values were nearly identical amounting to 168nm at the mean and the size distribution was unaffected by centrifugation as reflected by a PDI equal or less than 0.1. Interestingly, in general the zeta-potential values increased so that there is now any shielding effect of adsorbed carbohydrates not observed. Obviously, purification by centrifugation and washing resulted in removal of surface-associated carbohydrate.

Remarkably, the batches *chol5* and *chol7* containing carbohydrate in both phases suffered from low yield. The high viscosity of the medium impedes sedimentation of the nanoparticles during centrifugation so that only 15-20 mg of powder were recovered after purification and lyophilization, suggesting a limit on this technique. Considering this fact the batches chol 5 and chol 7 were not included in further studies.

### 5.2.3 Cholesterol-content of sugar-modified cholesterol-loaded Resomer® 503 Nps

The cholesterol loading of the batches was determined by HPLC/UV-detection as described in the methods section.

Sample	theoretical content (mg chol/100 mg formulation)	Practical content (mg chol/100 mg formulation)	E.E. %
chol 4	1	0.62 ( $\pm$ 0.12)	62 ( $\pm$ 9)
chol 6	1	0.59 ( $\pm$ 0.11)	60 ( $\pm$ 11)

Table 5.14. Entrapment efficiency of sugar-modified cholesterol-loaded Resomer® 503 Nps.

Notwithstanding the presence of sugar, both batches, *chol 4* and *chol 6*, showed an encapsulation efficiency of about 60%, very close to that of *chol 1a* (68%). This means that inclusion of carbohydrates within the PLGA-matrix does not affect the loading of cholesterol.

### 5.2.4. Use of low molecular weight PLGA

The second strategy adopted to form fast releasing cholesterol loaded nanoparticles was the use of a low molecular weight polymer. In particular, the Resomer® 502, Poly (D, L-lactide-co-glycolide) 50:50 with a viscosity in the range of 0.16-0.24 [dl/g], a molecular weight ranging from 7000 to 17000 Da and methyl ester endcaps was used. The batches were made from 50 mg PLGA Resomer® 502 and 0.5 mg cholesterol according to a PLGA-cholesterol ratio of 1:100 (w/w) and purified by centrifugation at 15000 or 17000 rpm for 10 minutes.

Sample	PLGA Resomer 502	Cholesterol	PLGA-chol ratio (w/w)	Purification
chol 8a	100 mg	1 mg	1:100	17000 rpm 10 min
chol 8b	100 mg	1 mg	1:100	15000 rpm 10 min

Table 5.15. Preparation parameters of cholesterol-loaded Resomer® 502 Nps.

### Pre centrifugation

Name	Z <sub>average</sub> ±SD (nm)	PDI	D10 (nm)	D50 (nm)	D90 (nm)	Zeta-potential (mV)	Z deviation
chol 8a	146 ± 8	0.08	104	151	222	-0.5	14.3
chol 8b	160 ± 9	0.08	111	167	255	-4.9	7.1

Table 5.16. Characteristics of cholesterol-loaded Resomer® 502 Nps immediately after preparation.

According to the data given in table 5.16. the characteristics of NPs made from PLGA Resomer® 502 were similar to those obtained for NPs made from PLGA Resomer® 503. Similarly, monomodal and monodisperse nanoparticles with 140-160 nm in size and lowest PDI were obtained.

The only apparent difference between the high and the low molecular weight PLGA preparations was the zeta-potential that was higher in case of the low molecular PLGA with values close to neutrality.

### Post centrifugation

Name	Z <sub>average</sub> ±SD (nm)	PDI	D10 (nm)	D50 (nm)	D90 (nm)	Zeta-potential (mV)	Z deviation
chol 8a	154 ±7	0.07	110	160	237	-3.3	8
chol 8b	164 ±9	0.08	118	170	248	-6.3	8.3

Table 5.17. Characteristics of cholesterol-loaded Resomer® 502 Nps after purification.

After the purification at both, 17000 rpm (chol 8a) and at 15000 rpm (chol 8b) rpm for 10 minutes, all the Nps were fairly redispersible without any change in size and size distribution. The zeta-potential was – 3 to -6 mV and lower than that of nanoparticles prepared from Resomer<sup>®</sup> 503, probably due to different surface exposure of the hydroxyl and ester groups of the polymer.

#### **Cholesterol-content of cholesterol-loaded Resomer<sup>®</sup> 502 Nps**

The contents were analyzed again by HPLC (as described above).

<b>sample</b>	<b>theoretical content (mg chol/100 mg formulation)</b>	<b>Practical content (mg chol/100 mg formulation)</b>	<b>E.E. %</b>
<b>chol 8a</b>	1	0.61 (±0.09)	60.9
<b>chol 8b</b>	1	0.76(± 0.12)	76.3

Table 5.18. Cholesterol-content of cholesterol-loaded Resomer<sup>®</sup> 502 Nps

In accordance with previous results, the encapsulation efficiency and the content were quite high with values higher than 60%.

## 6. Discussion

The aim of the present study was to evaluate the technological parameters for preparation of cholesterol-loaded PLGA nanoparticles by varying different formulation parameters during the nanoprecipitation process.

Firstly, the ratio between polymer and the drug cholesterol along with purification parameters were investigated.

Despite the high hydrophobicity of cholesterol, the use of different weight ratios of polymer and cholesterol did not significantly affect the process: in terms of the physicochemical parameters of all batches the mean particle size was about 200 nm with low polydispersity that makes the formulations suitable for i.v. administration. Slight differences in zeta-potential were observed regarding the data before and after purification. The batches prepared at a 1:100 ratio (cholesterol/PLGA, w/w) exhibited a decreased zeta-potential after the purification suggesting that considerable amounts of the surfactant PVA was removed from the particle surface during the centrifugation process making the polymer group more readily accessible. Especially in case of a batch prepared at a ratio of 1:10 (cholesterol/PLGA, w/w) a highly negative zeta potential was determined immediately after preparation which was not altered by subsequent purification. Considering also the high cholesterol-loading of about 2.3 mg / 100 mg nanoparticles, it is supposed that the drug is partially enclosed in the matrix structure as well as partially adsorbed at the surface. Moreover the presence of little amounts of probably adsorbed cholesterol facilitates redispersibility due to its surfactant-like properties as additionally confirmed by the SEM images of this batch showing no agglomerates.

To ensure a long-term stability of the nanoparticles, the batches were lyophilized yielding a dry powder most appropriate for long-term storage, transportation and reconstitution immediately before use. Nevertheless, as this process generates various stress conditions during freezing and drying, protectants are usually added to the formulation.

The most popular lyoprotectants reported in the literature for nanoparticles are the sugars trehalose, sucrose, glucose, and mannitol. The immobilization of nanoparticles within a glassy matrix of cryoprotectants can prevent their aggregation and protects them from degradation by avoiding the formation of large, uneven and dangerous ice crystals. Trehalose is one of the preferably used cryoprotectants for biomolecules as it offers many



advantages in comparison with the other sugars such as less hygroscopicity, absence of intramolecular hydrogen bonds allowing more flexible formation of hydrogen bonds with nanoparticles during freeze-drying, and finally very low chemical reactivity [Crowe 1996]). Accordingly, the results revealed that the addition of trehalose leads to fairly redispersible nanoparticles. Although literature suggests the use of the two or three-fold times amount of trehalose as compared to the amount of polymer, our results demonstrated that a polymer-trehalose ratio of 1:0,5 (w/w) is sufficient to ensure the redispersibility of cholesterol-loaded nanoparticles. Interestingly, nanoparticles prepared from higher amounts of cholesterol were well resuspendable even at lower sugar-polymer ratio.

Considering the loading efficiency of about 1 mg cholesterol /100 mg nanoparticles, it is easily conceivable that the major amount of cholesterol is dispersed within the polymer matrix and partly adsorbed at the surface. Consequently, the cholesterol structurally and physically modifies the nanoparticle concurrently with a flexible and improved dispersion of the drug.

Besides trehalose also PVA was evaluated as a cryoprotectant, which is well known to be adsorbed at the surface of PLGA nanoparticles. According to Murakami et al. the hydroxyl groups of PVA are attached to the acetyl group of PLGA via hydrophobic bonds [Murakami et al., 1999]. According to this model, PLGA nanoparticles made by the nanoprecipitation process using PVA as surfactant retain PVA even after purification by washing.

Previous data collected in our lab revealed that 5-8% of PVA remains adsorbed on PLGA nanoparticles even after purification by washing and centrifugation at 17000 rpm. This residual PVA, however, is not sufficient to stabilize 100-200 nm nanoparticles during the freeze drying as indicated by the disability of redispersion in water.

Accordingly, PVA has also been added after the purification as a cryoprotectant. The results confirmed the higher potency of PVA in comparison to trehalose, as all nanoparticle batches were well redispersible upon addition of the half amount of trehalose corresponding to a polymer/PVA ratio of 1:0.25 (w/w). Despite this clear evidence, trehalose should be preferred to PVA due to the surfactant activity, possible toxicity, action as cell membrane fluidity modifier (see review de Merlis et al., 2003), and possible modification of BBB permeability of PVA.

Nowadays, nanoparticles are considered as an efficacious drug carrier system, offering the potential advantages to stably encapsulate both, hydrophilic or lipophilic drugs, and to efficiently stabilize them in blood circulation. Moreover, they can be modified by

immobilizing biorecognitive molecules such as antibodies and peptides to accomplish targeted therapy. Besides the different advantages of nanoparticles like protection of encapsulated drugs and surface engineering for drug targeting, adjustment of the drug-loading encapsulation, degradation time and release kinetics, nanoparticles can be prepared from different kinds of polymers. In this context regarding the technological point of view, the type of polymer, the molecular weight and the use of additives could be considered as a strategy to modify the characteristics of nanoparticles.

Consequently, the second part of this study focused on the impact of different formulation parameters on possible changes in the matrix architecture to modify the release kinetics but concurrently preserving a good encapsulation yield.

Literature suggests that PLGA is able to assemble in closed matrix structures widely suitable for the encapsulation and stabilization of hydrophobic drugs [Barrichello et al., 1999; Derakhshandeh et al.]. In this kind of systems, a long term triphase release profile is commonly observed, consisting of an initial burst, a lag time with slow diffusion-controlled or without release depending on the molecular weight and end-capping of the polymer, and finally erosion-accelerated release. The initial burst of drug release is guided by the kind of drug, the drug concentration, and the polymer hydrophobicity. The next phases of the release profile comprise diffusion and degradation processes, unless it is still difficult to predict exactly the release-kinetics of a given drug. In generally, diffusion is the prevailing process until degradation of the polymer starts. The degradation of a polyester is a quite complicated process that involves bulk degradation by random hydrolytic scission of the backbone ester linkages and formation of initially insoluble, finally soluble oligomers and then soluble monomers in an autocatalytic manner (Gopferich et al., 1996). Moreover molecular weight also plays a key role in the degradation rate of polymer (Mittal et al., 2007).

Aiming to generate a more porous structure, sucrose modified nanoparticles were prepared. In our opinion the presence of even low amounts of glucose e.g. 0.8 mg /in 50 mg PLGA should provoke a less compact matrix structure due to the rapid diffusion of the sugar during the nanoparticles formulation. This type of nanoparticles is supposed to benefit from a faster diffusion due to accelerated interaction with the environment and a higher degradation rate. The experiments confirmed easy preparation of this type of nanoparticles from Resomer<sup>®</sup> 503 characterized by small size of less than 190 nm and high entrapment efficiency of 60%.

As the polymer molecular weight is one of the key factors affecting the degradation rate and the release profile, Resomer<sup>®</sup> 502 with lower molecular weight was also applied. The nanoparticles showed were 160nm in diameter and a relatively high zeta-potential, suggesting differences in polymer moieties now exposed at the surface. Unfortunately, these differences could not be confirmed by scanning electron microscopy probably due to limited magnification.

The molecular weight also reflects the hydrophilicity of the polymer since a decrease in molecular weight results in shorter polymer chain length. Keeping the amount of polymer constant, more polymer chains and consequently a higher number of hydrophilic groups are present that increase overall hydrophilicity and the accessibility of the medium. Although nanoparticles were prepared from polymer with lower molecular weight the high encapsulation efficiency of hydrophobic cholesterol in the range 60-70% was retained. Consequently it is suggested that the use of esterified polymer moiety acts as a balance between the low molecular chain length and the increase in hydrophobicity.

To confirm our hypotheses, an ex-vitro release study of cholesterol-loaded nanoparticle is carried out. Considering the low water solubility of cholesterol of 2µg/ml and the requirement of sink conditions during the experiment, we are now optimizing a highly sensitive detection method (GC-MS) eventually using low amounts of tween 80 to improve solubility of cholesterol in the acceptor compartment.



## 7. References

- Abbott, N. J. (2002). "Astrocyte-endothelial interactions and blood-brain barrier permeability." *Journal of Anatomy* 200(6): 629-638.
- Abbott, N. J., A. A. Patabendige, et al. (2010). "Structure and function of the blood-brain barrier." *Neurobiol Dis* 37(1): 13-25.
- Abbott, N. J., L. Ronnback, et al. (2006). "Astrocyte-endothelial interactions at the blood-brain barrier." *Nat Rev Neurosci* 7(1): 41-53.
- Jose A. Arcosa, Manuel Bernab  , and Cristina Otero, Different Strategies for Selective Monoacylation of Hexoaldoses in Acetone. *Journal of Surfactants and Detergents*, Vol. 1, No. 3 (July 1998)
- Ballabh, P., A. Braun, et al. (2004). "The blood-brain barrier: an overview: structure, regulation, and clinical implications." *Neurobiol Dis* 16(1): 1-13.
- Barichello, J.M., Morishita, M., Takayama, K., Nagai, T., 1999. Encapsulation of hydrophilic and lipophilic drugs in PLGA nanoparticles by the nanoprecipitation method. *Drug Dev. Ind. Pharm.* 25, 471–476.
- Cardoso, F. L., D. Brites, et al. (2010). "Looking at the blood-brain barrier: molecular anatomy and possible investigation approaches." *Brain Res Rev* 64(2): 328-363.
- Cattaneo E., Dysfunction of Wild-Type Huntingtin in Huntington disease; *News Physiol Science*; Vol.18, 34-37; 2003.
- Cattaneo E., Rigamonti D., Zuccato C., Le cause della corea di Huntington; *Le scienze*; 493-498; 2005.
- Y. Chen, L. Liu / *Advanced Drug Delivery Reviews* 64 (2012) 640–665
- Chen S., Le W., *Neuroprotective Therapy in Parkinson Disease*; *American Journal of Therapeutics*; 13, 445-457; 2006.
- Costantino L., Gandolfi F., Tosi G., Rivasi F., Vandelli M.A., Forni F., Peptide-derivatized biodegradable nanoparticles able to cross the blood–brain barrier; *Journal of Controlled Release*; 108 (1), 84-96; 2005.
- L.M. Crowe, D.S. Reid, J.H. Crowe, Is trehalose special for preserving dry materials? *Biophys. J.* 71 (1996) 2087–2093
- F. Danhier et al. / *Journal of Controlled Release* 161 (2012) 505–522
- C.C. DeMerlis, D.R. Schoneker. Review of the oral toxicity of polyvinyl alcohol (PVA). *Food and Chemical Toxicology* 41 (2003) 319–326
- K. Derakhshandeh , M. Erfan , S. Dadashzadeh . Encapsulation of 9-nitrocamptothecin, a novel anticancer drug, in biodegradable nanoparticles: Factorial design, characterization and release kinetics. *European Journal of Pharmaceutics and Biopharmaceutics* 66 (2007) 34–41
- C. Foged, B. Brodin, S. Frokjaer, A. Sundblad, Particle size and surface charge affect particle uptake by human dendritic cells in an in vitro model, *Int. J. Pharm.* 298 (2005) 315–322
- F. Franks, in: F. Franks (Ed.), *Water—a Comprehensive Treatise*, vol. 7, Plenum press, New York, 1982, pp. 215–238
- G  pferich, A.; *Mechanisms of Polymer Degradation and Erosion*; *Biomaterials*; 17 (1996) 103 - 114.
- Hawkins, B. T. and T. P. Davis (2005). "The blood-brain barrier/neurovascular unit

- in health and disease." *Pharmacol Rev* 57(2): 173-185.
- Hawkins, R. A., R. L. O'Kane, et al. (2006). "Structure of the blood-brain barrier and its role in the transport of amino acids." *Journal of Nutrition* 136(1 Suppl): 218S-226S.
  - Ikonen E. Cellular cholesterol trafficking and compartmentalization. *Nat Rev Mol Cell Biol* 2008;9:125–38.
  - V. Leoni et al. / *Neuroscience Letters* 494 (2011) 245–249
  - Wolfgang Löscher, Heidrun Potschka *Progress in Neurobiology* Volume 76, Issue 1, May 2005, Pages 22–76
  - Mittal G, Sahana DK, Bhardwaj V, Ravi Kumar MN . *J Control Release*. 2007 May 14; 119(1): 77-85. Pub 2007 Feb 3. Estradiol loaded PLGA nanoparticles for oral administration: effect of polymer molecular weight and copolymer composition on release behavior in vitro and in vivo.
  - Murakami et al., *Int Journal of pharamaceutics* 187 (1999) 143-152
  - Myers R.H., *Huntington's disease genetics; NeuroRx*; **1** (2), 255–62; 2004.
  - Pardridge, W. M. (1999). "Blood-brain barrier biology and methodology." *J Neurovirol* 5(6): 556-569
  - Persidsky, Y., S. H. Ramirez, et al. (2006). "Blood-brain barrier: structural components and function under physiologic and pathologic conditions." *J Neuroimmune Pharmacol* 1(3): 223-236.
  - Petty, M. A. and E. H. Lo (2002). "Junctional complexes of the blood-brain barrier: permeability changes in neuroinflammation." *Prog Neurobiol* 68(5): 311-323.
  - F.W. Pfrieger / *Biochimica et Biophysica Acta* 1610 (2003) 271–280
  - F.W. Pfrieger, N. Ungerer / *Progress in Lipid Research* 50 (2011) 357–371
  - M.J. Pikal, Mechanisms of protein stabilization during freeze-drying and storage: the relative importance of thermodynamic stabilization and glassy state relaxation dynamics, in: L. Rey, J.C. May (Eds.), *Freeze-Drying/Lyophilization of Pharmaceutical and Biological Products*, vol. 96, Marcel Dekker, New York, 1999, pp. 161–198.
  - Reiner, A., Albin, R.L., Anderson, K.D., D'Amato, C.J., Penney, J.B., Young, A.B., 1988. Differential loss of striatal projection neurons in Huntington disease. *Proc. Natl. Acad. Sci. U.S.A.* 85, 5733–5737.
  - Rosas, H.D., Koroshetz, W.J., Chen, Y.I., Skeuse, C., Vangel, M., Cudkowicz, M.E., Caplan, K., Marek, K., Seidman, L.J., Makris, N., Jenkins, B.G., Goldstein, J.M., 2003. Evidence for more widespread cerebral pathology in early HD: an MRI-based morphometric analysis. *Neurology* 60, 1615– 1620.
  - H.M. Shubar, I.R. Dunay, S. Lachenmaier, M. Dathe, F.N. Bushrab, R. Mauludin, R.H. Müller, R. Fitzner, K. Borner, O. Liesenfeld, The role of apolipoprotein-E in uptake of atovaquone into the brain in murine acute and reactivated toxoplasmosis, *J. Drug Target*. 17 (2009) 257–267.
  - M. Simionescu, A. Gafencu, F. Antohe, Transcytosis of plasma macromolecules in endothelial cells: a cell biological survey, *Microsc. Res. Tech.* 57 (2002) 269–288.
  - Tosi G., Costantino L., Rivasi F., Ruozi B., Leo E., Vergoni A.V., Tacchi R., Bertolini A., Vandelli M.A., Forni F., Targeting the central nervous system: In vivo experiments with peptide- derivatized nanoparticles loaded with Loperamide and Rhodamine-123; *Journal of Controlled Release*; 122, 1-9; 2007.
  - Tosi G., Costantino L., Ruozi B., Forni F., Vandelli M.A., Polymeric nanoparticles for the drug delivery to the central nervous system; *Expert Opinion drug delivery*; 5, 155-174; 2008.

- M. Valenza, E. Cattaneo / *Progress in Neurobiology* 80 (2006) 165–176
- R.L. VanGilder et al. / *Pharmacology & Therapeutics* 130 (2011) 239–247
- J.K. Vasir, V. Labhasetwar, Quantification of the force of nanoparticle–cell membrane interactions and its influence on intracellular trafficking of nanoparticles, *Biomaterials* 29 (2008) 4244–4252.
- Vergoni A.V., Tosi G., Tacchi R., Vandelli M.A., Bertolini A., Costantino L., Nanoparticles as drug delivery agents specific for CNS: in vivo biodistribution; *Nanomedicine: Nanotechnology, Biology and Medicine*; 5, 369-377; 2009.
- S.V. Vinogradov, E.V. Batrakova, A.V. Kabanov, Poly (ethylene glycol)-polyethyleneimine nanogel particles: novel drug delivery systems for antisense oligonucleotides, *Colloids Surf. B Biointerfaces* 16 (1999) 291–304.
- S. Wohlfart et al. / *Journal of Controlled Release* 161 (2012) 264–273
- H.L. Wong et al. / *Advanced Drug Delivery Reviews* 64 (2012) 686–700
- C. Zuccato, E. Cattaneo / *Progress in Neurobiology* 81 (2007) 294–330

## 8. Deutsche Zusammenfassung

Die therapeutische Gabe von Cholesterol spielt vor allem bei neurodegenerativen Erkrankungen, wie Chorea Huntington, Alzheimer und Parkinson eine wichtige Rolle, wie mehrere Studien belegen.

Das größte Problem bei der Therapie dieser Erkrankungen stellt die Blut-Hirn-Schranke dar, da diese weitgehend den Transport von aktiven Substanzen wie Cholesterol oder andere Wirkstoffen ins Zentralnervensystem unterbindet.

Daher gelten nicht invasive Therapien mit Arzneiformen wie Nanopartikeln, die die Blut-Hirn-Schranke überwinden können, als zukunftsweisend.

Im Rahmen dieser Arbeit wurden unterschiedliche Nanopartikel-Chargen mit dem Ziel hergestellt möglichst große Mengen an Cholesterol einzukapseln. Dabei wurde versucht, die Parameter für die Nanopräzipitation als Herstellungsprozess zu optimieren. Zusätzlich wurden unterschiedliche Polymer/Cholesterol-Verhältnisse und Aufreinigungsprozesse untersucht, um die geeignetste Produktionsmethode zu finden.

Die höchste Verkapselungseffizienz wiesen die Nanopartikel mit einem Polymer-Cholesterol Verhältnis von 1:100 (G/G) auf, wobei keine signifikanten Unterschiede nach unterschiedlichen Aufreinigungsparametern beobachtet wurden.

Die beste Möglichkeit Nanopartikel aufzubewahren stellt die Lyophilisation dar. Jedoch muss auch eine problemlose Redispergierbarkeit gewährleistet sein. Als mögliche und etablierte Cryo- und Lyoprotektoren wurden PVA und Trehalose untersucht.

Obwohl PVA bessere Eigenschaften zeigte, ist aufgrund der fehlenden Unbedenklichkeit bei der humanen Gabe Trehalose der Vorzug zu geben.

Weiterführende Studien an der Universität Mailand bewiesen, dass diese Nanopartikel zwar in der Lage sind, die Blut-Hirn-Schranke zu überwinden, aber aufgrund ihrer hohen Stabilität Cholesterol nicht in therapeutisch relevanten Mengen freisetzen.

Daher wurden zwei Modifikationen untersucht, um die Freisetzungsrates zu erhöhen: erstens wurden Nanopartikel aus einem niedermolekularen Polymer (Resomer<sup>®</sup> 502) hergestellt und zweitens wurden Formulierungen mit Zucker als Porenbildner produziert. Hierbei wurde der Zucker entweder nur der organischen oder beiden Phasen während der Herstellung zugesetzt. Durch den Zusatz des hydrophilen Hilfsstoffes sollte der Eintritt von Wasser und die Quellbarkeit des Polymers erhöht werden, was letztlich in einer



beschleunigten Freisetzung von Cholesterol resultieren sollte Um diese Theorie zu bekräftigen sind jedoch noch Freisetzungsuntersuchungen und gleichzeitig eine Entwicklung einer sensitiveren Quantifizierungsmethode für Cholesterol notwendig, die während meines Aufenthaltes nicht mehr möglich waren.

## 9. CURRICULUM VITAE

### PERSONAL DETAILS

Name	Birgit Gstöttenbauer
Nationality	Austria
Date of Birth	25.05.1987

.....

### EDUCATION AND QUALIFICATIONS

Time periode	from 1. march till 30. june 2012
Name of the qualitifcation	Erasmus student in Modena, Italy
Name and type of organisation providing education and training	University of Modena TeFaRi Research group laboratory work for the thesis

Time periode	from january 2010 till june 2010
Name of the qualification	Erasmus student in Helsinki, Finland
Name and type of organisation providing education and training	University of Helsinki, Faculty of pharmacy Division of social pharmacy

Time periode	from october 2005 till october 2012
Name of the qualification	Master of pharmacy
Name and type of organisation providing education and training	University of Vienna, Faculty of pharmacy

Time periode	from october 1997 till june 2005
Name of the qualification	graduation
Name and type of organisation providing education and training	Petrinum, catholic private school Petrinumstraße 12, 4040 Linz, Austria

.....

## EMPLOYMENT HISTORY

Time periode	from 1. july till 31.july 2007
Profession or function	trainee in the laboratory
Name and adress of employer	Kwizda Pharma Poschacherstraße 37, 4020 Linz
Time periode	from 1. august till 31.august 2009
Profession or function	trainee in a pharmacy
Name and adress of employer	Hans Sachs Apotheke Währinger Straße 84, 1180 Vienna
Time periode	since 18. February 2012
Profession or function	trainee in a pharmacy
Name and adress of employer	Apotheke der Barmherzigen Brüder Taborstraße 16, 1020 Vienna

.....

## FURTHER EDUCATION

### PROFESSIONAL QUALIFICATIONS

Courses besides main lectures	drug targeting, Prof. Gabor nanoparticels in pharmaceutical technology, Prof. Wirth & Prof. Gabor cell cultures in the pharmaceutical technology, Prof. Wirth
I.T. Proficiency	Good working knowledge of Microsoft Word, Power Point, Excel
Languages	German (native) English (fluent) Italian (intermediate) Latin (intermediate) French (intermediate)